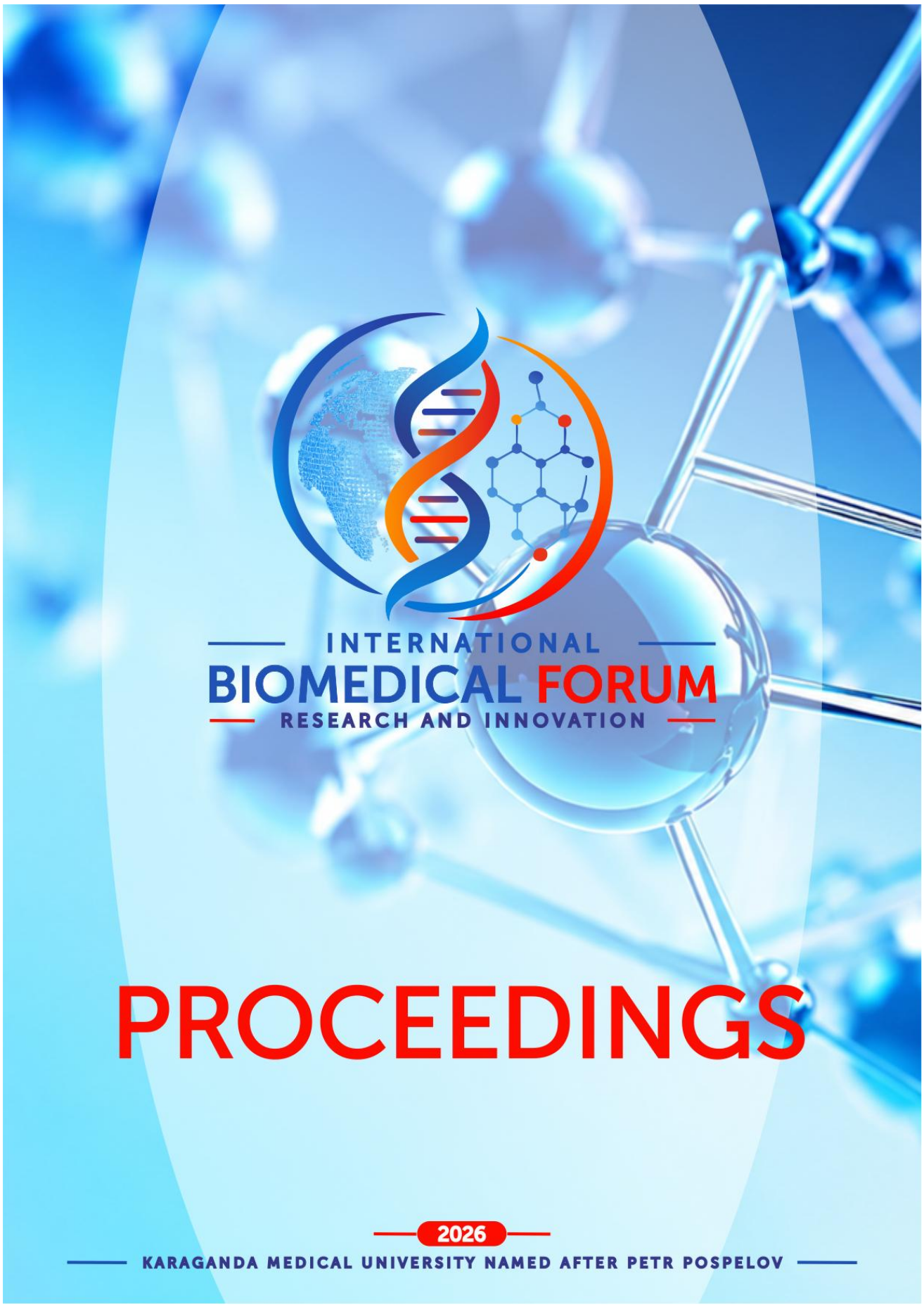

INTERNATIONAL

BIOMEDICAL FORUM

RESEARCH AND INNOVATION

PROCEEDINGS

2026

KARAGANDA MEDICAL UNIVERSITY NAMED AFTER PETR POSPELOV

MINISTRY OF HEALTH OF THE REPUBLIC OF KAZAKHSTAN
«KARAGANDA MEDICAL UNIVERSITY NAMED AFTER P. POSPELOV» NC JSC
«KSMU ALUMNI ASSOCIATION» PA

II International Biomedical Forum Research and Innovation

PROCEEDINGS

Karaganda
October 22 – 23, 2026

UDC 61(574.31)(063)
LBC 51/58
R 45

R 45 Research and Innovation: Proceedings of II International Biomedical Forum. - Karaganda, 2026. – 46 p.

The Proceedings contains materials and abstracts of reports by participants of the II International Biomedical Forum dedicated to advanced research and innovations in the field of life sciences. The issue includes works by leading scientists, experts, as well as young researchers and doctoral students, reflecting the current state and prospects for the development of biomedical science.

The issue is aimed at researchers, biologists, pharmacologists, practicing physicians, teachers of medical universities, as well as undergraduates, doctoral students and students specializing in biomedicine and biotechnology.

UDC 61(574.31)(063)
LBC 51/58

General editorship by Professor B. N. Kosherova

Editorial Board
D. Klyuyev, I. Kadyrova, V. Ricklefs, Zh. Dauletkaliyeva, A. Kalina, N. Aleshina, D. Gissa, A. Bukeyeva, A. Lavrinenko, D. Silishchev, A. Tukenova, Ye. Serbo

© «Karaganda Medical University named after P. Pospelov» NC JSC, 2026

A. A. Aitkenova[1], G. A. Atazhanova[1]

BIOLOGICAL EFFECTS OF AN ULTRASOUND-ASSISTED ETHANOLIC EXTRACT OF *IRIS SCARIOSA* L. IN YEAST AND *ARTEMIA SALINA* BIOASSAYS

[1]«Karaganda Medical University named after P. Pospelov» NC JSC (100008, Republic of Kazakhstan, Karaganda c., Gogolya str., 40; e-mail: info@qmu.kz)

Introduction. Preliminary screening of plant extracts helps identify their biological effects and guides subsequent pharmacological investigations. The *Artemia salina* bioassay provides an initial assessment of toxicity, while a yeast assay using *Saccharomyces cerevisiae* offers complementary information on changes in metabolic activity. These models examine different biological responses and therefore require separate interpretation. Reduced foam formation is an indirect indicator of altered yeast metabolism, whereas larval mortality reflects toxicity within the brine shrimp model. Neither endpoint alone establishes cytotoxicity in mammalian cells or the safety of an extract. Evaluating both responses can provide a basis for selecting more specific assays for further investigation.

Aim. To assess the effects of an ultrasound-assisted ethanolic extract of *Iris scariosa* L. on the metabolic activity of *Saccharomyces cerevisiae* and the survival of *Artemia salina* larvae.

Materials and methods. An *I. scariosa* extract obtained by ultrasound-assisted extraction using 70% ethanol (IS-U-70) was investigated at the Department of Biomedicine, Karaganda Medical University. The present abstract reports the initial series of screening experiments. In the yeast assay, the rate of foam formation during exposure to the extract was assessed relative to the control and used as an indirect indicator of cellular metabolic activity. In the *A. salina* bioassay, the extract was tested at concentrations of 1 and 0.25 mg/mL. Doxorubicin was included as a reference compound at concentrations of 1, 0.5, and 0.25 mg/mL. Larval survival was assessed after 10, 20, and 30 minutes of exposure. Experiments were performed in triplicate. Mortality percentages were calculated as 100% minus the corresponding survival percentages.

Results. Exposure to the extract reduced the rate of foam formation in *S. cerevisiae* compared with the control. This finding is consistent with reduced metabolic activity but does not independently demonstrate yeast cell death. In the *A. salina* bioassay, survival at an extract concentration of 1 mg/mL decreased from 90 to 70% over the observation period, corresponding to an increase in mortality from 10 to 30%. At 0.25 mg/mL, survival ranged from 80 to 100%, corresponding to mortality of 0 – 20%. No larval mortality was observed in the control group. Mortality therefore occurred at both extract concentrations in the initial experimental series. At 1 mg/mL, mortality increased with exposure duration. The survival range reported for 0.25 mg/mL does not establish the absence of toxicity or demonstrate a consistent concentration-dependent response across all observation times.

Conclusion. The ultrasound-assisted ethanolic extract of *I. scariosa* affected both biological endpoints examined in the initial experimental series. Extract exposure reduced yeast foam formation and caused mortality among *A. salina* larvae. At 1 mg/mL, larval mortality reached 30% during the observation period. These preliminary findings support further investigation of the extract's biological activity and toxic properties. Additional viability assays, longer exposure periods, and studies in mammalian cell models are required to characterize its cytotoxic effects and assess its safety profile.

Key words: *Iris scariosa*; ethanolic extract; ultrasound-assisted extraction; *Saccharomyces cerevisiae*; *Artemia salina*; toxicity

M. M. Arzakulova[1], D. A. Tokashbayeva[2], D. E. Omertayeva[3]

METABOLOMIC BIOMARKERS OF SEVERE CHRONIC HYPERTENSION IN PREGNANCY: ASSOCIATIONS BETWEEN PURINE INTERMEDIATES AND BETA-2-MICROGLOBULIN

[1]«Karaganda Medical University named after P. Pospelov» NC JSC (100008, Republic of Kazakhstan, Karaganda c., Gogolya str., 40; e-mail: info@qmu.kz)

Introduction. Severe chronic arterial hypertension (CAH) in pregnancy carries a higher risk of maternal and fetal complications, yet it is still assessed almost entirely from blood pressure and routine laboratory tests. The metabolic and immune changes that accompany it are far less well described. Purine intermediates come from nucleotide catabolism and respond to hypoxia and oxidative stress. Beta-2-microglobulin (B2M), a component of major histocompatibility complex class I molecules, may instead reflect immune activation and renal stress. Measured together, the two may say more about a patient than either does alone. We therefore compared B2M and purine intermediates in erythrocytes and plasma between third-trimester women with severe CAH and normotensive controls, related them to clinical parameters, and looked for markers associated with severe CAH.

Materials and methods. We reviewed 58 women with singleton pregnancies at 28–40 weeks who were treated in the pregnancy pathology departments of Perinatal Centres No. 1 and No. 2 in Karaganda between December 2017 and December 2020; the design was retrospective and cross-sectional. Twenty-nine had severe CAH, defined as systolic blood pressure ≥160 mmHg or diastolic blood pressure ≥110 mmHg at two or more consecutive visits. The remaining 29 were apparently healthy women with no chronic disease, systolic blood pressure below 140 mmHg and diastolic below 90 mmHg. Multiple pregnancy, gestational diabetes, acute infection, autoimmune or oncological disease and any drug affecting purine metabolism were grounds for exclusion. Venous blood was drawn in the morning after an 8-hour fast. B2M was measured by enzyme-linked immunosorbent assay; guanine, hypoxanthine, adenine, xanthine and uric acid were quantified in erythrocytes and plasma by high-performance liquid chromatography, every sample in duplicate. Groups were compared with the Mann–Whitney U test and associations examined with Spearman correlations. Generalized linear models and propensity score matching were used to allow for relevant clinical variables, binary logistic regression to identify markers associated with severe CAH, and receiver operating characteristic (ROC) analysis to judge how well they separated the groups. The local ethics committee of Karaganda Medical University approved the study (Protocol No. 33 of 3 January 2018) and all data were anonymized.

Results. Gestational age was similar in the two groups, but the women with CAH were older and of higher parity. B2M was higher in CAH than in controls (2.64 vs 1.58 mg/L; $p<0.001$). Erythrocyte guanine (395.2 vs 309.6 nmol/L; $p=0.002$), erythrocyte uric acid (111.7 vs 80.5 nmol/L; $p=0.004$) and plasma hypoxanthine (252.6 vs 181.3 nmol/L; $p=0.012$) also differed between the groups. Adjustment for age, gestational age and parity left the differences in B2M and erythrocyte guanine significant. B2M correlated with erythrocyte guanine (rho=0.45; $p<0.001$), with erythrocyte uric acid (rho=0.39; $p=0.003$) and with systolic blood pressure (rho=0.41; $p=0.002$). In the adjusted logistic model, B2M was associated with severe CAH (odds ratio 2.1; 95% confidence interval 1.3–3.4; $p=0.002$), as was erythrocyte guanine (odds ratio 1.8; 95% confidence interval 1.1–2.9; $p=0.018$). The area under the ROC curve was 0.84 for B2M, 0.79 for erythrocyte guanine and 0.87 for the two markers combined.

Conclusion. Women with severe CAH had higher B2M, erythrocyte guanine, erythrocyte uric acid and plasma hypoxanthine than normotensive controls. B2M and erythrocyte guanine remained associated with severe CAH after adjustment for the main clinical variables, and the two

together discriminated best in this dataset. Markers of immune activation and of purine turnover thus varied alongside the clinical severity of hypertension, although a cross-sectional design says nothing about the order in which they change. The results are exploratory: the study was retrospective and single-centre, the sample small, and pregnancy outcomes were not followed. Cut-off values, and the question of whether these markers add anything to clinical monitoring or to the prediction of maternal and fetal complications, need prospective multicentre work.

Key words: beta-2-microglobulin; purine metabolism; guanine; uric acid; chronic arterial hypertension; pregnancy

E. B. Biyaliev[1], S. A. Ivasenko[1], I. Korona-Glowniak[2], A. B. Marchenko[1]

DEVELOPMENT OF A NEW ANTIBACTERIAL AGENT FOR THE TREATMENT OF PNEUMOCOCCAL DISEASES BASED ON BIOLOGICALLY ACTIVE SUBSTANCES OF *THYMUS CREBRIFOLIUS* KLOK.

[1]«Karaganda Medical University named after P. Pospelov» NC JSC (100008, Republic of Kazakhstan, Karaganda c., Gogolya str., 40; e-mail: info@qmu.kz)
[2]Medical University of Lublin (20-093, Poland, Lublin, Chodzki Street, 1)

Introduction. Pneumococcus (*Streptococcus pneumoniae*) is included in the list of high-priority pathogens posing the greatest threat to human health according to the World Health Organization. Pneumococcus is the causative agent of pneumococcal infection, a group of infectious diseases in humans that primarily affect children. Elderly people are also considered a risk group. According to WHO estimates, 1.6 million people die worldwide each year from diseases caused by pneumococcus, including 0.7–1 million children under 5 years of age. In 2027, pneumococcal diseases such as pneumonia, bacteremia, and meningitis are expected to remain a serious public health issue in Kazakhstan, despite vaccination efforts. A promising approach to solving this problem is the search for and development of new antimicrobial agents, including those of plant origin, with fundamentally different mechanisms of action capable of overcoming existing forms of microbial resistance. The aim of the study is to develop a new antibacterial agent for the treatment of pneumococcal diseases based on biologically active substances of *Thymus crebrifolius* Klok., an endemic plant of the flora of Kazakhstan.

Materials and methods. The aerial part of the endemic plant *Thymus crebrifolius* was collected in the wild in the Republic of Kazakhstan, in the vicinity of the city of Zhezkazgan in the Ulytau Mountains, during the full flowering phase. The plant material was extracted with 96% ethanol and 70% ethanol using ultrasound. The composition of polyphenolic compounds in the extract was studied using LC-UV-MS. The antibacterial activity of the extracts was evaluated by the microdilution method against the reference microorganism from the American Type Culture Collection (ATCC) - *Streptococcus pneumoniae* ATCC 49619.

Results. Ultrasound-assisted extraction of *Thymus crebrifolius* plant material was carried out using 96% ethanol or 70% ethanol at an ultrasound frequency of 28 kHz or 40 kHz. LC-UV-MS analysis revealed differences in the qualitative composition and quantitative content of phenolic compounds in the obtained extracts. In the 96% ethanol extracts, 15 phenolic compounds were identified and quantitatively determined; the main components were rosmarinic acid (12.75 and 14.38 mg/g), apigenin-7-*O*-glucuronide (11.10 and 13.29 mg/g), and luteolin-7-*O*-glucoside (8.98 and 10.10 mg/g). In the 70% ethanol extracts, 11 phenolic compounds were identified; the dominant components were luteolin-7-*O*-glucoside (99.90 and 109.00 mg/g), rosmarinic acid (28.62 and 30.98 mg/g), apigenin-7-*O*-glucuronide (15.88 and 16.34 mg/g), and naringenin (22.68 and 24.84 mg/g). It was established that 96% ethanol extracts of *Thymus crebrifolius* exhibit

pronounced bactericidal activity against *Streptococcus pneumoniae* at a concentration of 1.25 mg/mL.

Conclusion. The dry 96% ethanol extract of *Thymus crebrifolius* obtained using ultrasound at 40 kHz can be considered as an active pharmaceutical ingredient for the development of a new antibacterial agent for the treatment of pneumococcal diseases.

Key words: *Thymus crebrifolius* Klok.; extract, polyphenolic compounds; antimicrobial activity; *Streptococcus pneumoniae*

Z. Darmani[1], M. Shahzaib[2], M. H. Modabber[3], S. Haider[4], M. Myrzakhanova[1]

THE EFFECT OF VIRTUAL REALITY ON STUDENTS' ATTENTION AND VISUAL MEMORY

[1]Shokan Ualikhanov, Kokshetau University (020000, Republic of Kazakhstan, Akmola Region, Kokshetau c., Abay Street, 76; e-mail: university@shokan.edu.kz)
[2]Allama Iqbal Medical College (Allama Iqbal Medical College, Jinnah Hospital, Faisal Town, Lahore, Punjab, Pakistan.; e-mail: principal@aimc.edu.pk)
[3]Kabul University of Medical Sciences «Abu Ali Ibn Sina» (Faculty of Medicine, Kabul University of Medical Sciences «Abu Ali Ibn Sina», Kabul, Afghanistan; e-mail: info@kums.edu.af)
[4]FMH College of Medicine and Dentistry (Lahore, Pakistan; e-mail: info@fmhcmd.edu.pk)

Introduction. Virtual reality (VR) is increasingly used in medical education to create immersive, interactive learning environments that increase student engagement and knowledge retention. Although enthusiasm for VR teaching tools is growing, evidence remains limited that VR provides measurable cognitive benefits compared with traditional two-dimensional (2D) instruction. Furthermore, individual differences among learners (such as their level of technological comfort, sense of presence, immersion, and susceptibility to cybersickness) may significantly affect how students respond to VR-based teaching. To integrate VR into medical curricula effectively and evidence-based, it is important to establish both VR's relative effectiveness compared with 2D learning and the role of individual technology-related factors. This study aimed to compare, among medical students, attention, visual memory, sense of presence, engagement, and overall cognitive performance between those who finished a VR-immersive learning session and those who completed an equivalent 2D-control session, and also to investigate the associations between technology-related experiential factors and the cognitive outcomes reported by the students.

Materials and methods. This randomized controlled trial study involved 85 medical students, most of whom were in their fourth or sixth year of study. The participants were assigned randomly into two groups: one received immersive learning via a head-mounted display, and the other was given the same educational material in a 2D-control setup displayed on a standard screen. After the learning session, each participant filled out a structured self-report questionnaire which evaluated five areas – attention, visual memory, sense of presence, mental engagement, and an overall cognitive score. The questionnaire also included questions relating to technological aspects, such as participants' level of comfort with the technology, whether they felt overwhelmed during the session, and any symptoms of cybersickness. The main analysis compared the five cognitive and experiential results between the VR-immersive group and the 2D-control group by using statistical tests suitable for the type of data distribution. As a further, exploratory analysis, Spearman's rank correlation coefficient was applied to look at the relationships between the technology-related factors (technological comfort, feeling overwhelmed, and cybersickness) and the cognitive and experiential outcome measures. For all the analyses, a p-value less than 0.05 was regarded as statistically significant.

Results. The main comparison between the VR-immersive group and the 2D-control group revealed no statistically significant differences among the five outcomes measured: attention (p=0.90), visual memory (p=0.20), sense of presence (p=0.50), engagement (p=0.68), and the total cognitive score (p=0.59). In contrast, the exploratory correlation analysis found several significant associations between technology-related factors and cognitive outcomes, regardless of group assignment. Technological comfort was positively correlated with attention (rho=0.344, p=0.0014) and with sense of presence (rho=0.393, p<0.001). Cybersickness was negatively correlated with sense of presence (rho= -0.222, p=0.042). The feeling of being overwhelmed during the learning session was positively correlated with attention (rho=0.380, p<0.001), engagement (rho=0.383, p<0.001), and the total cognitive score (rho=0.396, p<0.001). These findings indicate that although there was no significant difference between the two learning methods, individual differences in how students experienced and interacted with the technology were meaningfully linked to their reported cognitive outcomes.

Conclusion. One VR-immersive learning session did not result in statistically significant differences in attention, visual memory, sense of presence, engagement, or overall cognitive performance when compared to an equivalent 2D-control condition. Nevertheless, various technological and experiential factors were found to be significantly linked to several cognitive and learning-related outcomes: higher technological comfort was associated with improved attention and a stronger sense of presence, cybersickness was related to a lower sense of presence, and feeling overwhelmed was connected with greater attention, higher levels of engagement, and higher total cognitive scores. The results indicate that the educational value of VR in medical training may rely less on the modality itself and more on the way in which individual students interact with and experience the technology. It is therefore necessary to carry out further controlled studies that use objective cognitive measures, involve larger samples, and include repeated exposure to VR to clarify these relationships and to guide the effective of VR into medical education.

Key words: Virtual Reality; attention; Visual Memory; Cognitive Performance, Digital Technology

D. Duisegali[1], M. Fadin[1], S. Yegorov[1], V. Strochkov[2], A. Lavrinenko[3], V. Parakhina[4], N. Sandybayev[2]

IMPACT OF EMPIRIC ANTIBIOTICS ON MICROBIAL DIVERSITY AND ANTIMICROBIAL RESISTANCE IN PNEUMONIA

[1]Department of Biological and Biomedical Sciences, Nazarbayev University School of Medicine (Astana, Kazakhstan)
[2]Kazakhstan-Japan Innovation Centre, Kazakh National Agrarian Research University (Almaty, Kazakhstan)
[3]Research Laboratory, «Karaganda Medical University named after P. Pospelov» NC JSC (100008, Republic of Kazakhstan, Karaganda c., Gogolya str., 40; e-mail: info@qmu.kz)
[4]Department of Internal Medicine, «Karaganda Medical University named after P. Pospelov» NC JSC (100008, Republic of Kazakhstan, Karaganda c., Gogolya str., 40; e-mail: info@qmu.kz)

Introduction. Empiric antibiotic therapy (EAT) is essential for the management of community-acquired pneumonia (CAP), yet broad-spectrum antibiotic exposure may disrupt the respiratory microbiota and select for antimicrobial resistance. CAP patients are typically started on EAT within hours of admission, before microbiological results are available. Empiric treatment may involve several broad-spectrum antibiotics selected according to disease severity, comorbidities, and local epidemiology, with therapy later adjusted based on the patient's clinical response and microbiological results. Although necessary for initial CAP management, such treatment can also affect the respiratory microbiota by reducing colonization resistance, promoting opportunistic pathogens, and altering the antimicrobial resistance gene (ARG) profile. Previous studies have provided limited information on how antibiotics affect the respiratory microbiome and antimicrobial resistance. Some focused only on

the upper respiratory tract, while others lacked samples collected before antibiotic treatment, detailed information on antibiotic exposure, or included patients who were already receiving antibiotics at baseline. However, early EAT-associated changes in the respiratory microbiome and resistome of CAP patients remain insufficiently characterized.

Materials and methods. In this prospective observational study, 90 hospitalized patients with CAP provided paired expectorated sputum samples before EAT initiation and immediately before treatment termination or de-escalation (post-EAT; median interval, 3 days). Samples were analyzed using 16S rRNA gene profiling, targeted next-generation sequencing of respiratory pathogens and antimicrobial resistance genes (ARGs), and conventional microbiological culture.

Results. Post-EAT, Shannon diversity significantly declined among lower respiratory tract inhabitants, ARG reservoir taxa, Gram-positive taxa, and facultative anaerobes (FDR≤0.030). Among targeted respiratory pathogens, *Haemophilus influenzae* abundance decreased (p=0.039), whereas *Klebsiella pneumoniae* increased approximately threefold (p=0.037). Baseline phenotypic resistance ranged from 69% to 95% and generally increased following EAT. Aminoglycoside ARG diversity and richness increased, while beta-lactam ARG diversity and richness decreased. Trimethoprim ARG richness increased, whereas lincosamide ARG richness decreased (all FDR<0.05). ARG abundance was positively associated with *K. pneumoniae* and *Pseudomonas aeruginosa*. Within-class ARG expansion was associated with exposure to trimethoprim (p=0.004) and tetracyclines (p=0.024).

Conclusion. EAT was associated with rapid changes in clinically relevant respiratory microbial communities and with antibiotic class-specific shifts in the resistome. The increase in potentially pathogenic bacteria such as *K. pneumoniae*, together with changes in ARG diversity and richness, suggests that even a short course of empiric therapy can affect both the respiratory microbiome and resistance profile. These changes may reflect not only the direct effects of antibiotics, but also indirect selection of resistant bacterial populations and resistance genes. Overall, the findings highlight the broader impact of empiric therapy and support careful use of broad-spectrum antibiotics, particularly in settings with a high prevalence of antimicrobial resistance.

Key words: community-acquired pneumonia; empiric antibiotic therapy; respiratory microbiome; respiratory resistome; antimicrobial resistance; antimicrobial resistance genes; targeted next-generation sequencing; antimicrobial stewardship

A. V. Hramyka[1], S. A. Zvezhinskiy[1], A. A. Baroski[1], A. V. Davidyan[2]

USE OF MACHINE LEARNING TO PREDICT RECURRENCE AFTER THIRD VENTRICULOSTOMY

[1]Belarusian state medical university (220083, Republic of Belarus, Minsk c., Dzerzhinsky av., 83; e-mail: bsmu@bsmu.by)
[2] Republican Scientific and Practical Center of Neurology and Neurosurgery (220114, Republic of Belarus, Minsk s. F. Sckarini 24 av.; e-mail: info@neuro.by)

Introduction. Hydrocephalus is a heterogeneous disease caused by impaired production, circulation, or resorbtion of cerebrospinal fluid (CSF) and manifested by dilation of CSF-containing spaces with specific clinical presentation. Endoscopic third ventriculostomy (ETV) is a minimally invasive CSF-draining intervention that creates an alternative CSF outflow pathway; it is used in hydrocephalus of various etiologies. Despite the absence of an implantable shunt system and relatively low invasiveness, the risk of recurrence persists and depends on etiology, age, previous operations, anatomical features, and condition of the CSF pathways. Predicting recurrence is challenging due to the multifactorial nature and non-linearity of pathophysiological

mechanisms. Morphometric parameters of the third ventricle may reflect the state of CSF dynamics and the anatomy of this region, which justifies their consideration as potential predictors of outcome. Traditional statistical methods (logistic regression, prognostic scales) focus primarily on assessing individual variables and linear effects, which limits accuracy in complex interactions of features. Machine learning allows building models optimized for generalization to new data. Validation is mandatory: splitting into training and test sets, cross-validation, nested cross-validation for hyperparameter tuning, and external validation on an independent population; it evaluates discrimination, calibration, and clinical usefulness of the model, reducing the risk of optimistic bias. Regularization (L1, L2, Elastic Net) limits excessive model complexity and prevents overfitting. Feature selection is performed using Recursive Feature Elimination (RFE) and Binary Gravitational Search Algorithm (BGSA). The combination of cross-validation, regularization, and feature selection creates prerequisites for personalized prediction of hydrocephalus recurrence risk after ETV.

Materials and methods. A retrospective analysis was performed on the data of 85 medical records of adult patients treated at the Healthcare Institution "Republican Scientific and Practical Center of Neurology and Neurosurgery" between January 2022 and September 2025. The inclusion criteria for the study were: a history of ETV and the availability of preoperative and postoperative MRI scans in sagittal and axial projections obtained no more than 3 months before and after surgery, respectively. For each patient, sex and age at diagnosis were assessed. Separately, the chance of a favorable ETV outcome was calculated using the Kulkarni score. This score takes into account the patient's age, etiology of hydrocephalus, and history of prior ventriculoperitoneal shunting (VPS) and, on this basis, assigns the patient a specific percentage probability of a favorable ETV outcome. Morphometric parameters were obtained by dividing a certain linear or angular value on the preoperative image by the corresponding postoperative value.

Results. When selecting predictors using the BGSA algorithm, the following combination of features was obtained: rACTC, LT_preoperative. The ROC-AUC value was 0.506, sensitivity – 40%, specificity – 87.5%. When applying the RFE algorithm, the following features were selected: sex, ETVSS, rACTC, Ztoma, Adhesions, TVF_preoperative, LT_preoperative, TVF_postoperative. The ROC-AUC value was 0.625, sensitivity – 60%, specificity – 81.2%.

Conclusion. These results may be due to the low proportion of patients with disease recurrence and the small number of patients in the sample. It is necessary to increase the number of patients in the database, introduce additional morphometric parameters, and improve model training with the possible implementation of alternative algorithms: SHAP, Boruta, and decision tree.

Key words: hydrocephalus; third ventriculocisternostomy; machine learning; BGSA; RFE

M. S. Izerskaya[1], L. A. Dildabekova[1]

ENZYMES AS BIOLOGICAL CATALYSTS AND THEIR SIGNIFICANCE IN THE CHILD'S ORGANISM

[1]JSC «South Kazakhstan Medical Academy» (160019, Republic of Kazakhstan, Shymkent, Al-Farabi Square, 1; e-mail: info@skma.kz)

Introduction. Enzymes are biological macromolecules that accelerate biochemical reactions and make the continuous metabolism of living cells possible. Their activity is especially important during childhood, when the organism undergoes intensive growth, differentiation of tissues and formation of functional systems. The aim of this work was to describe the biological role of enzymes and to summarize their significance for the growth, energy metabolism, digestion, antioxidant protection and development of the child's organism. Understanding age-related features of enzymatic activity is relevant for the interpretation of laboratory parameters and for the recognition of conditions associated with impaired metabolism.

Materials and methods. A review and synthesis of educational and biomedical literature concerning enzyme structure, catalytic mechanisms, classification and physiological functions were performed. Particular attention was paid to enzymes involved in carbohydrate, lipid and protein metabolism, digestive processes, nucleic acid synthesis and antioxidant defense. Age-related characteristics of enzymatic systems were considered in relation to normal growth and development. The reviewed information was systematized according to the main metabolic functions of enzymes in the developing organism.

Results. The literature analysis showed that enzymes are essential regulators of biochemical reactions in the developing child's organism. Their catalytic activity supports coordinated energy production, nutrient digestion, biosynthesis and cellular protection. Digestive enzymes, including amylases, proteases and lipases, participate in the hydrolysis of carbohydrates, proteins and lipids, providing substrates for absorption and tissue growth. Enzymes of glycolysis, the citric acid cycle and oxidative phosphorylation contribute to ATP production, which is particularly important during periods of intensive growth and development. Enzymatic systems also participate in DNA and RNA metabolism, protein synthesis and formation of cell structures. Antioxidant enzymes, including superoxide dismutase, catalase and glutathione peroxidase, contribute to protection of cells from excessive oxidative stress. The reviewed data indicate that enzyme activity has age-dependent characteristics; therefore, biochemical enzyme markers in children should be interpreted using age-appropriate reference intervals. Changes in aminotransferase, amylase and lipase activity may accompany pathological processes involving the liver, muscles or pancreas, but these indicators require interpretation together with clinical findings and other laboratory parameters. Adequate nutrition and sufficient availability of vitamins and trace elements are important for normal enzyme synthesis and function because many enzymes require cofactors or coenzymes.

Conclusion. Enzymes are fundamental regulators of biochemical reactions and therefore have a direct significance for the growing child. They ensure digestion, energy production, biosynthesis, cellular protection and coordinated metabolism. Age-related differences in enzymatic activity should be considered when evaluating biochemical tests in pediatric practice. Knowledge of enzymatic mechanisms helps explain normal development and provides a basis for understanding metabolic disorders. Further study of age-specific enzyme activity may contribute to more accurate interpretation of laboratory findings and to the improvement of approaches to pediatric care.

Key words: enzymes; biological catalysis; child development; metabolism; digestive enzymes; oxidative stress

A. T. Kalkenova[1], A. Zh. Mendibayeva[1], D. V. Shestakov, K. T. Shakeyev[2], A. K. Zeinidenov[1]

SPECTROSCOPIC ANALYSIS OF SALIVA SAMPLES USING FLUORESCENCE AND FTIR SPECTROMETRY FOR CERVICAL CANCER DETECTION

[1]Karaganda Buketov National Research University (100024, Republic of Kazakhstan, Karaganda c., Universitetskaya str. 28; e-mail: office@karnu-buketov.edu.kz)
[2]«Karaganda Medical University named after P. Pospelov» NC JSC (100008, Republic of Kazakhstan, Karaganda c., Gogolya str., 40; e-mail: info@qmu.kz)

Introduction. Cervical cancer (CC) ranks among the leading positions in female reproductive system malignancies worldwide, creating an urgent need to develop fundamentally novel, express, highly sensitive, non-invasive, and cost-effective screening technologies. Traditional cytological and histological screening methods are frequently associated with procedural invasiveness, patient discomfort, and high labor intensity. In recent years, biological fluids, particularly saliva, have been actively investigated as a promising alternative, serving as a unique non-invasive diagnostic substrate. Saliva contains a wide range of soluble biomolecules (proteins, peptides, enzymes, metabolites, electrolytes) that sensitively respond to any pathological shifts and systemic metabolic alterations in the body caused by the development of malignant neoplasms. The aim of this study was a comprehensive investigation of the spectral characteristics of saliva samples from healthy laboratory mice and animals with an experimental cervical cancer model using high-sensitivity fluorescence and Fourier-transform infrared (FTIR) spectroscopy.

Materials and methods. The experimental part of the study was performed on biological saliva samples obtained from a control group of healthy mice and a group of animals with tumor process induction (cervical cancer model). The recording of luminescence spectra of the studied biosamples was carried out using a high-precision DW-F98 Fluorescence Spectrophotometer within a wavelength range of 420 to 750 nm. Infrared absorption spectra (IR spectra) in the mid-IR range were recorded using an FSM-2202 FTIR spectrometer within a wavenumber range of 4000 to 500 cm^{-1}.

Results. A detailed comparative analysis of the luminescence spectra recorded using the DW-F98 instrument revealed essential and reliable qualitative and quantitative differences between the control and experimental groups. The spectral curves of saliva samples from healthy mice are characterized by a smooth, stable, and monotonic profile with the dominance of a main band maximum in the narrow zone of 430-450 nm and a smoothed weak shoulder around 505-510 nm, while the relative fluorescence intensity is stably maintained within the range of 0.00 to 1.00. A completely different pattern is demonstrated by the saliva spectra of mice with developing cervical cancer, a profound structural rearrangement of the fluorescence profile is observed here. In the 430-500 nm range, the appearance of complex split multi-component peaks is recorded, the maximum luminescence intensity values increase up to 1.25, and the peak in the 510-520 nm region acquires a pronounced sharpened character. These changes are caused by a systemic alteration in the concentrations and conformational state of endogenous biomolecular fluorophores in saliva (such as NAD(P)H coenzymes, flavin complexes, structural proteins, products of enhanced lipid peroxidation, and tumor-associated metabolites). The obtained data are fully supported by the results of FTIR spectrometry using the FSM-2202 instrument. Infrared spectra of healthy samples demonstrate a stable absorption profile with classical absorption bands: a broad band of O–H/N–H stretching vibrations of hydroxyl and amino groups in the region of about 3300 cm^{-1}, as well as distinct analytical bands of Amide I (about 1650 cm^{-1}) and Amide II (about 1540 cm^{-1}), reflecting the native structure of the peptide skeleton of saliva proteins, with optical density values within 0.35-0.55. Conversely, the IR spectra of tumor samples reveal pronounced pathological deviations: a noticeable shift in the baseline absorption, redistribution of intensities

and peak shifts in the characteristic «fingerprint region» (1500-500 cm^{-1}), as well as severe changes in the spectral intervals of stretching and bending vibrations of lipids and carbohydrate components (1200-900 cm^{-1}) are observed. These spectral markers reflect profound alterations in the protein-lipid profile of saliva during oncogenesis, caused by cellular metabolism disruption and tissue degradation.

Conclusion. The combined and integrated application of fluorescence spectroscopy (based on the DW-F98 instrument) and FTIR spectrometry (based on the FSM-2202 instrument) has proved its high efficacy for the reliable detection of specific biochemical and structural changes in saliva associated with the development of cervical cancer. The established features of luminescence intensity changes and shifts in IR spectra can serve as reliable spectral biomarkers. The developed approach opens wide prospects for creating fundamentally new, express, highly sensitive non-invasive screening systems for early diagnostics and monitoring of antitumor therapy efficacy in clinical practice.

Key words: cervical cancer; saliva; fluorescence spectroscopy; FTIR spectroscopy; biomedical diagnostics

A. Kazbekova[1], S. Sagadinov[1], S. Yegorov[1]

DETECTION OF BACTERIOPHAGE SIGNATURES IN TARGETED SEQUENCING DATA FROM SPUTUM SAMPLES OF PATIENTS WITH PNEUMONIA IN KAZAKHSTAN

[1]Nazarbayev University (010000, Republic of Kazakhstan, Astana c., Kabanbay Batyr ave., 53; e-mail: altynay.kazbekova@nu.edu.kz)

Introduction. Bacteriophages infect bacteria and may provide complementary information about bacterial populations in clinical specimens. Their recovery from sequencing data depends on specimen preparation, library design, and the specificity of computational identification. Existing targeted next-generation sequencing (NGS) data from sputum samples of pneumonia patients in Kazakhstan provide an opportunity to investigate whether phage-associated sequences can be recovered from an assay designed primarily for bacterial detection. Unlike untargeted metagenomic sequencing, a bacterial-targeted assay cannot be assumed to represent the complete sputum virome. This study aims to assess whether credible bacteriophage signatures can be identified in direct sputum libraries and whether matched cultured bacterial data can support interpretation of putative host relationships.

Materials and methods. The project collection comprises 148 sequencing datasets: 52 direct sputum NGS datasets, 48 cultured NGS datasets, and 48 culture-derived whole-genome sequencing datasets. Direct sputum libraries constitute the primary screening group. Cultured datasets provide supplementary bacterial context where specimen and patient links can be verified; they are not included in the denominator for sputum phage detection. Preliminary read-level screening was performed against a curated phage database. The validation framework includes read quality assessment and filtering, human-sequence subtraction, duplicate handling, and competitive searches against bacterial and human references. Candidate matches are evaluated for alignment length, sequence identity, sequence complexity, and specificity. Independent verification includes broader nucleotide database searches using BLAST+. Where sufficient overlapping reads permit assembly, geNomad is used to investigate viral identity, while CheckV assesses suitable assembled viral contigs rather than individual short reads. Final detection criteria will specify minimum read support and alignment requirements before supported signatures are summarized. Available background controls and computational controls will be used to investigate

false matches. Related prophage sequences in matched bacterial genomes may support putative host assignments but cannot establish the presence of free phage particles in sputum.

Results. Preliminary screening of all 52 direct sputum libraries identified multiple putative bacteriophage-associated matches. Frequently matched references included Streptococcus phages Phi-SsUD.1, phiJH1301-2, phi-m46.1, and phiNJ3. Additional matches involved phage references associated with Pseudomonas, Acinetobacter, Staphylococcus, and Moraxella. These findings generated candidates for further investigation but did not establish confirmed phage identities or bacterial host assignments. Biologically unexpected references, including Dickeya phage phiDP10.3 and Listeria phage WIL-3, were matched across all 52 libraries. Their widespread occurrence raises concerns about conserved regions shared among references, ambiguous short-read alignments, or common technical background. The preliminary matches are therefore being investigated through independent sequence checks and assembly-based viral identification using geNomad and CheckV. The number of libraries with validated phage signatures has not yet been established. Current findings demonstrate the need to distinguish initial reference matches from supported detections before drawing biological conclusions.

Conclusion. Preliminary analysis identified candidate bacteriophage signatures in targeted sputum sequencing data from pneumonia patients in Kazakhstan. However, frequent unexpected reference matches indicate that read-level database matching alone is insufficient to confirm phage identity. Competitive searches against non-phage references, explicit support thresholds, and independent validation are necessary for reliable interpretation. The study will assess whether existing bacterial-targeted libraries retain informative phage sequences and define the limitations of their reuse for this purpose. Failure of candidates to pass validation would indicate limited detection feasibility under the applied assay and analytical conditions, rather than absence of bacteriophages from the original specimens. Validated signatures, if recovered, could guide subsequent investigation using untargeted or phage-enriched sequencing. These preliminary findings do not establish a comprehensive sputum virome, phage prevalence among pneumonia patients, or clinical diagnostic accuracy.

Key words: bacteriophages; pneumonia; sputum; targeted sequencing; bioinformatics; Kazakhstan

G. K. Kelgali[1], I. E. Aldabergen[1], A. Zh. Mendibayeva[1], A. K. Aimukhanov[1], A. K. Zeinidenov[1]

SPECTRAL-LUMINESCENT CHARACTERISTICS OF SALIVA IN LUNG CANCER DIAGNOSIS

[1]Karaganda Buketov National Research University (100024, Republic of Kazakhstan, Karaganda c., Universitetskaya str. 28; e-mail: office@karnu-buketov.edu.kz)
[2]«Karaganda Medical University named after P. Pospelov» NC JSC (100008, Republic of Kazakhstan, Karaganda c., Gogolya str., 40; e-mail: info@qmu.kz)

Introduction. Lung cancer remains one of the leading causes of cancer-related mortality, and its prognosis is strongly influenced by the stage at which the disease is detected. This makes the development of accessible, non-invasive approaches for identifying disease-associated biochemical changes an important research objective. Saliva is a promising biological fluid for optical analysis because it can be collected easily and contains proteins, metabolites and endogenous fluorophores whose spectral characteristics may reflect physiological and pathological processes. The aim of this study was to assess whether absorption and fluorescence

characteristics of saliva differ between patients with lung cancer and healthy volunteers, and to evaluate the potential value of these optical parameters for non-invasive screening.

Materials and methods. The study included saliva samples from 59 patients with primary morphologically confirmed lung cancer and 31 healthy volunteers. Samples were obtained at the Multidisciplinary Hospital No. 3 in Karaganda, Kazakhstan. Before optical measurements, saliva was centrifuged at 10,000 rpm to remove cellular material and debris. Absorption spectra were recorded in the ultraviolet–visible spectral range. Steady-state fluorescence spectra and fluorescence-decay kinetics were also measured. The analysis focused on the intrinsic optical properties of saliva and on differences between the cancer and control groups. The measured parameters included optical density at selected wavelengths, fluorescence emission features and fluorescence lifetime.

Results. The optical measurements revealed clear differences between saliva samples from patients with lung cancer and healthy volunteers. The optical density of saliva in the cancer group was higher across the measured spectral range. At 280 nm, the optical density was approximately 1.91 times that of the control group, while in the 320-400 nm region the difference was approximately 1.67-2.0-fold. The absorption spectra of the cancer group were broader and their spectral peak was shifted relative to the control samples. These changes may reflect differences in the concentration and composition of salivary chromophores, including proteins and other ultraviolet-absorbing components. Fluorescence measurements also showed group-dependent features. The overall fluorescence intensity of saliva from patients with lung cancer was approximately 1.7 times higher than that of the control group. An emission band around 505 nm, associated in the study with oxidized flavins, was observed, while an additional band near 614 nm was detected in samples from the cancer group. This additional emission was attributed to endogenous porphyrins and may indicate changes in the biochemical composition or metabolic state of saliva. The presence of this band is particularly noteworthy because it provides a spectral feature that can be considered alongside absorption and fluorescence intensity rather than relying on a single measurement. Time-resolved measurements provided an additional distinction between the groups. The mean fluorescence lifetime increased from 1.32 ns in control saliva to 1.89 ns in saliva from patients with lung cancer. At the emission wavelength of 614 nm, the reported lifetime was 0.42 ns for controls and 1.26 ns for the cancer group. Fluorescence lifetime reflects the excited-state dynamics of emitting molecules and can be influenced by their molecular environment and interactions. Therefore, the differences observed in lifetime may complement steady-state spectral measurements and help characterize changes in endogenous salivary fluorophores. Taken together, the increased optical density, higher fluorescence intensity, appearance of an emission band near 614 nm and longer fluorescence lifetime form a set of distinguishable optical features associated with the lung cancer group. These findings suggest that combined analysis of absorption, emission spectra and fluorescence-decay kinetics may provide more informative characterization of saliva than any single parameter alone.

Conclusion. This study identified differences in the absorption and fluorescence properties of saliva from patients with lung cancer compared with healthy volunteers. The cancer group showed increased optical density, approximately 1.7-fold higher fluorescence intensity, an additional emission band near 614 nm and an increased mean fluorescence lifetime. These results indicate that intrinsic optical characteristics of saliva contain measurable features associated with lung cancer and support further investigation of saliva-based spectroscopy as a non-invasive screening approach. The findings should be interpreted as preliminary: larger independent cohorts and validation against relevant clinical variables are needed before the method can be considered for clinical application.

Key words: saliva; lung cancer; optical absorption; fluorescence spectroscopy; fluorescence lifetime; non-invasive diagnostics

O. I. Khan[1], A. A. Olkhov[1, 2, 3], S. G. Karpova[2]

NON-WOVEN FIBROUS MATERIALS BASED ON POLYLACTIDE AND POLYCAPROLACTONE FOR MEDICAL APPLICATIONS

[1]Plekhanov Russian University of Economics (115054, Russian Federation, Moscow c., Stremyanny lane, 36; e-mail: rector@rea.ru)
[2]Emanuel Institute of Biochemical Physics of Russian Academy of Sciences (119334, Russian Federation, Moscow c., Kosygina str., 4; e-mail: ibcp@sky.chph.ras.ru)
[3]N. N. Semenov Federal Research Center for Chemical Physics Russian Academy of Sciences (119991, Russian Federation, Moscow c., Kosygina str., 4; e-mail: icp@chph.ras.ru)

Introduction. The advancement of modern regenerative medicine, tissue engineering, and targeted drug delivery systems creates an urgent need for the development of next-generation biocompatible and biodegradable materials. Among the wide range of materials, biodegradable polymers specifically polycaprolactone (PCL) and polylactide (PLA) attract particular attention from researchers. PCL is characterized by high elasticity, ease of processing, and availability. However, its high hydrophobicity hinders initial cell adhesion, and its biodegradation rate in the body is often too slow for many biomedical applications. PLA is a promising biodegradable biopolymer that has been actively studied over the past two decades. Its monomer, lactic acid, is produced via fermentation from renewable plant sources such as starch and sugar. Therefore, PLA is considered a desirable alternative to traditional petroleum-based polymers. The aim of the work is to create non-woven fibrous materials for medical applications.

Materials and methods. We used bio-based PLA with an average viscosity molecular weight of 190 kDa and polyε-caprolactone pellets (Mw~80 kDa) PCL, melting temperature 60 °C. Ultra-thin PLA/PCL fibers were produced by electrospinning [on an EFV-1 single-capillary lab scale unit. The capillary diameter is 0.2 mm. The distance between the capillary and the precipitation electrode was 20 cm. The voltage was 17 kV. Feed solutions of PLA/PCL in chloroform were prepared at different polymer ratios. The total concentration of polymers in the solution was 7 wt%. Stirring was carried out using a magnetic stirrer at 50 °C. The morphology of nonwoven samples was studied using a laser 3D microscope. An MTT assay was performed to determine cytotoxicity. PCL/PLA polymer compositions in various ratios were placed in a 96-well plate. MCF7, SW620, U87MG breast cancer cells (5,000 cells) were seeded into the wells in 200 µL of RPMI-1640 culture medium. The MCF7 cells were incubated with the polymer compositions for 72 hours. After 72 hours, 20 µL of MTT (3-(4,5-dimethylthiazol-2-yl)-2,5-diphenyltetrazolium bromide) was added to the cells. After 3.5 hours, once formazan crystals had formed, the MTT-containing medium was removed, and DMSO was added to dissolve the crystals. Following dissolution, absorbance was measured using a spectrophotometer at a wavelength of 540 nm. Cell viability was calculated as the ratio of the mean value for the polymer-treated samples (experimental group) to the mean value for wells not containing polymer compositions (control group).

Results. Fibers based on polymer blends exhibit multiple bead-like thickenings. The size of these thickenings ranges from 10 to 40 µm. Their formation is attributed to the rheological characteristics of PLA and PCL within the blends. The stretching dynamics of the polymer solutions appear to be complicated by relaxation processes in the polymer phases at the interface and by differing surface tension values resulting from the polymers' molecular characteristics. This is indicated by the diameters of the individual polymers: PLA fibers have a diameter of 5–15 µm, while PCL fibers measure 2-5 µm. The diameters of the cylindrical fibers in the blends fall within the 2–12 µm range. The cytotoxicity of the obtained materials also varied: the pure materials exhibited low toxicity, with cell survival rates of 68.3% (MCF7), 108.1% (SW620), and 76.4% (U87MG) for PLA, and 79.9% (MCF7), 86.4% (SW620), and 86.8% (U87MG) for PCL. Adding

PCL to PLA reduced SW620 cell survival to levels comparable to those observed with pure PCL, with survival rates ranging from 81% to 88% ($p=0.29$ for the 20% PLA/80% PCL composite compared to pure PCL). In U87MG cell cultures, blending the two polymers resulted in enhanced cytotoxic properties; the material composed of 70% PLA and 30% PCL was the most cytotoxic, yielding a cell survival rate of 50.6% (though this did not reach statistical significance, with $p=0.75$ and $p=0.37$ compared to PLA and PCL, respectively). Increased PLA cytotoxicity was also observed in MCF7 cell cultures upon the addition of PCL, with the effect being concentration-dependent: the material composed of 10% PLA and 90% PCL caused 43% cell death ($p<0.05$ compared to PLA and PCL). These results demonstrate that blending PLA with PCL enhances the cytotoxic properties of PLA, suggesting potential for their application in antitumor therapy.

Conclusion. MTT assay results demonstrate that blending PLA with PCL enhances the cytotoxic properties of PLA, suggesting potential for their application in antitumor therapy. In biodegradable PLA/PCL fibers, the observed structural features and segmental mobility alterations should have an essential influence on diffusivity, the profile of controlled release, and mechanical behavior, which is the subject of further investigations designated for biomedical implementation.

Key words: polylactide; polycaprolactone; electrospun fibers; MTT assay

O. K. Kosherov[1], S. A. Ivasenko[1]*, T. Kacergius[2]

ANTIBACTERIAL AND ANTIBIOFILM ACTIVITY OF *THYMUS CREBRIFOLIUS* KLOK. EXTRACTS AGAINST *STREPTOCOCCUS MUTANS*

[1]«Karaganda Medical University named after P. Pospelov» NC JSC (100008, Republic of Kazakhstan, Karaganda, Gogolya st., 40; e-mail: info@qmu.kz)
[2]Vilnius University (03101, Lithuania, Vilnius, M. K. Ciurlionio st., 21)

Introduction. *Streptococcus mutans* (*S. mutans*) is one of the best-recognized etiological agents involved in the pathogenesis of dental caries, an infectious disease that remains highly prevalent worldwide. The resistance of this bacterium to antimicrobial agents is associated with its ability to form biofilms on tooth surfaces and produce organic acids (acidogenicity) from sucrose within the biofilm, contributing to tooth decay. In addition, biofilm-associated bacteria have been reported to be up to 1000-fold more resistant to antimicrobial agents than planktonic bacteria. Therefore, the development of new pharmaceutical agents to inhibit *S. mutans* biofilm formation and acidogenicity is important. The aim of this study was to investigate the antibacterial and antibiofilm activities of *Thymus crebrifolius* extracts against *Streptococcus mutans*, an endemic plant species of the flora of Kazakhstan.

Materials and methods. The herb of *Thymus crebrifolius* was collected from the wild in the Republic of Kazakhstan, in the vicinity of the city of Zhezkazgan in the Ulytau Mountains, during full flowering. *Thymus crebrifolius* extracts were obtained by twofold ultrasonic extraction of plant material at ultrasound frequencies of 28 and 40 kHz using 70% ethanol, followed by evaporation of the extractant on a rotary evaporator. The *Streptococcus mutans* UA159 strain (ATCC 700610) was cultured in Todd-Hewitt broth (THB) under anaerobic conditions (95% N_2 and 5% CO_2) at 37 °C for 18 h before the experiments. The minimum inhibitory concentration (MIC) was determined by the broth microdilution method. The antibiofilm activity of the obtained extracts (TC-2-28 and TC-2-40) against *Streptococcus mutans* was evaluated in vitro using crystal violet staining.

Results. The study showed that the obtained extracts TC-2-28 and TC-2-40 exhibited antibacterial activity against *Streptococcus mutans* with an MIC of 12.5 mg/mL. The tested extracts inhibited *S. mutans* biofilm formation in a medium containing 1% sucrose, which is a

major inducer of biofilm formation in *S. mutans*, and exhibited a dose-dependent effect. Extract TC-2-28 at concentrations of 2, 3, 4, 5, and 6 mg/mL reduced *S. mutans* biofilm formation by 19, 47, 67, 96, and 97%, respectively, compared with untreated bacteria ($p<0.05$) in Todd-Hewitt broth containing 1% sucrose. Extract TC-2-40 at concentrations of 3, 4, 5, 6, and 7 mg/mL reduced *S. mutans* biofilm formation by 14, 42, 56, 88, and 96%, respectively, compared with untreated bacteria ($p<0.05$) in Todd-Hewitt broth containing 1% sucrose.

Conclusion. The *Thymus crebrifolius* extracts TC-2-28 and TC-2-40 exhibited antibacterial activity against *Streptococcus mutans* with an MIC of 12.5 mg/mL. The *Thymus crebrifolius* extract TC-2-28 showed comparatively greater inhibitory activity; at a concentration of 6 mg/mL, it reduced *S. mutans* biofilm formation by 97%. These results support the potential use of TC-2-28 as a natural ingredient in products intended for the treatment and/or prevention of dental caries.

Key words: *Thymus crebrifolius* Klok.; antibacterial activity; biofilm inhibition; *Streptococcus mutans*

G. Manish[1]

REGIONAL TRENDS IN MULTIDRUG/RIFAMPICIN-RESISTANT TUBERCULOSIS: ANALYSIS OF WHO DATA FROM 2015 – 2024

[1]«Karaganda Medical University named after P. Pospelov» NC JSC (100008, Republic of Kazakhstan, Karaganda, Gogolya st., 40; e-mail: manishgaur2022@gmail.com)

Introduction. Drug-resistant tuberculosis continues to be an important public health problem and remains a challenge for TB control programmes. MDR/RR-TB is particularly important because treatment is more complex and the disease can place a greater burden on health systems. Although the global estimated burden of MDR/RR-TB has decreased in recent years, this improvement may not have occurred equally in all parts of the world. Looking at regional changes can therefore provide a clearer picture of where the burden has decreased and where it has remained stable or increased.

Aim. To assess changes in the estimated MDR/RR-TB burden between 2015 and 2024 and compare the trends across the six WHO regions. The study also aimed to identify regions with the largest reductions and regions where the estimated burden showed little improvement or an increase.

Materials and methods. WHO MDR/RR-TB burden estimates for 2015–2024 were used for this secondary-data analysis. Country-level estimates were grouped according to the six WHO regions: African, Americas, Eastern Mediterranean, European, South-East Asian, and Western Pacific Regions. Available country estimates were summed within each region for every year to obtain regional estimates. The global estimate was also calculated from the available regional data. The percentage change from 2015 to 2024 was calculated for each region and globally. Linear regression was used to examine the direction and statistical significance of the overall trend in the aggregated global estimates during the study period. The analysis was based on publicly available WHO estimates and did not involve collection of personal or clinical patient data.

Results. The aggregated global estimate decreased from 591,967 in 2015 to 391,916 in 2024, corresponding to a 33.8% decrease. The largest reduction was observed in the African Region, where the estimate decreased from 153,707 to 57,087 (62.9%). The Eastern Mediterranean Region decreased from 36,310 to 19,197 (47.1%). The European Region decreased by 39.6%, while the Western Pacific Region decreased by 36.6% between 2015 and 2024. In contrast, the Americas showed an increase from 12,482 to 14,166 (13.5%). The South-East Asia Region also showed a small increase, from 143,915 to 148,527 (3.2%). Overall, the regional results showed that the

direction and size of change were not uniform. Linear regression demonstrated a significant decreasing trend in the aggregated global estimates, with a slope of approximately −21,122 estimated cases per year ($p<0.001$).

Conclusion. The estimated MDR/RR-TB burden decreased globally between 2015 and 2024, but the pattern differed substantially between WHO regions. Several regions showed marked reductions, while the Americas and South-East Asia showed little improvement or an increase over the study period. These differences indicate that progress in reducing the estimated MDR/RR-TB burden has not been uniform. Regional trends should therefore be considered when assessing TB control progress and when deciding where additional public health attention may be needed. Because the analysis uses WHO estimates rather than individual patient data, the findings should be interpreted as population-level estimates and not as exact numbers of diagnosed cases.

Key words: MDR/RR-TB; tuberculosis; drug resistance; WHO; epidemiology; regional trends

M. M. Mirsaidullaev[1], N.S. Mamasoliev[2]

TRANSNOSOLOGICAL COMORBIDITY IN REPRODUCTIVE-AGE WOMEN WITH ISCHEMIC HEART DISEASE: RESULTS OF POPULATION SCREENING IN NAMANGAN

[1]Impuls Medical Institute, Namangan Branch (Republic of Uzbekistan, Namangan Region, Namangan c., Otamirzayev stre., 1 K; e-mail: info@impulsmi.uz)
[2]Andijan State Medical Institute (Republic of Uzbekistan, Andijan, Yu. Otabekov str., 1; e-mail: info@adti.uz)

Introduction. Ischemic heart disease (IHD) in women of reproductive age may remain underrecognized because of atypical or minimally symptomatic clinical manifestations and the frequent coexistence of chronic noncommunicable diseases. Multimorbidity can complicate diagnostic interpretation, increase pharmacological burden and reduce the effectiveness of preventive interventions. Therefore, population-based identification of transnosological comorbidity, defined as the coexistence of diseases belonging to different nosological classes, may improve risk stratification and early prevention in this population.

Aim. To assess the prevalence and structure of transnosological comorbidity among women of reproductive age with ischemic heart disease identified during population screening in Namangan.

Materials and methods. A population-based epidemiological study included 4,990 women aged 15 – 49 years examined at the Central Polyclinic of Namangan city. The sample comprised 571 women aged 15 – 19 years, 1,420 aged 20 – 29 years, 1,638 aged 30 – 39 years and 1,361 aged 40 – 49 years. The examination program included a standardized questionnaire, clinical assessment, blood pressure and anthropometric measurements, 12-lead resting electrocardiography, ultrasonography, and laboratory testing including total cholesterol, triglycerides, glucose, serum iron and troponin. IHD was diagnosed using combined clinical and electrocardiographic criteria. Chronic noncommunicable comorbidities were identified by clinical, laboratory and instrumental assessment. Transnosological comorbidity was categorized as absent, presence of 1–2 chronic noncommunicable diseases, or presence of ≥3 diseases. Statistical analysis was performed using IBM SPSS Statistics 26 with χ^2 tests, Fisher's exact test, relative risk estimates and 95% confidence intervals; $p<0.05$ was considered statistically significant.

Results. IHD was identified in 155 of 4,990 screened women, corresponding to a prevalence of 3.1%. Among the women with IHD, 26 had acute IHD and 129 had chronic IHD. Transnosological comorbidity was absent in only 17 women (11.0%), whereas 131 women

(84.5%) had 1 – 2 chronic noncommunicable diseases and 7 women (4.5%) had ≥3 comorbid diseases. Thus, 89.0% of women with IHD had at least one chronic noncommunicable comorbidity. In acute IHD, the corresponding distribution was 15.4% without comorbidity, 80.8% with 1 – 2 diseases and 3.8% with ≥3 diseases. In chronic IHD, these proportions were 10.1%, 85.3% and 4.7%, respectively. The distribution of transnosological comorbidity did not show a statistically significant difference between acute and chronic IHD groups ($p>0.05$). In age-stratified analysis, 30 – 39-year-old women with IHD showed a similarly high burden: 84.6% had 1 – 2 comorbid diseases and 7.7% had ≥3. Among women aged 40–49 years, 84.1% had 1 – 2 comorbid diseases and 4.0% had ≥3, confirming that multimorbidity is already common before the end of reproductive age.

Conclusion. Population screening demonstrated that IHD in women aged 15 – 49 years is rarely an isolated condition: almost nine of ten women with detected IHD had at least one additional chronic noncommunicable disease. The predominance of 1 – 2 concomitant diseases in both acute and chronic IHD supports the need for integrated screening rather than disease-specific case finding. Assessment of comorbidity should be incorporated into cardiovascular risk stratification, preventive counseling and treatment planning for reproductive-age women, with particular attention to women aged 30 – 49 years.

Key words: ischemic heart disease; reproductive-age women; transnosological comorbidity; screening; chronic noncommunicable diseases; preventive cardiology

M. M. Mirsaidullaev[1], N. S. Mamasoliev[2]

COMORBID PROFILE AND PHARMACOTHERAPEUTIC FEATURES OF ISCHEMIC HEART DISEASE IN REPRODUCTIVE-AGE WOMEN

[1]Impuls Medical Institute, Namangan Branch (Republic of Uzbekistan, Namangan Region, Namangan c., Otamirzayev stre., 1 K; e-mail: info@impulsmi.uz)
[2]Andijan State Medical Institute (Republic of Uzbekistan, Andijan, Yu. Otabekov str., 1; e-mail: info@adti.uz)

Introduction. Ischemic heart disease (IHD) in women of reproductive age is characterized not only by the clinical form of the disease but also by a substantial burden of concomitant cardiovascular and chronic noncommunicable disorders. The presence of several diseases in one patient complicates therapeutic decision-making, increases the potential for drug interactions and polypharmacy, and requires an individualized approach to long-term treatment. For this reason, simultaneous assessment of the comorbid profile and the actual structure of treatment is important for improving the safety and rationality of medical care in reproductive-age women with IHD.

Aim. To characterize the structure of cardiovascular and chronic noncommunicable comorbidity and to assess the main pharmacotherapeutic approaches in reproductive-age women with IHD in order to identify priorities for optimizing treatment and pharmacological monitoring.

Materials and methods. The results of examination of 4,990 women aged 15 – 49 years were analyzed. IHD was detected in 155 women, including 26 cases of acute IHD and 129 cases of chronic IHD. The analysis included cardiovascular comorbid conditions, chronic noncommunicable diseases associated with IHD, and the treatment approaches used in the study population. Treatment was classified as non-pharmacological, pharmacological, or surgical. The distribution of comorbid conditions and treatment modalities was evaluated according to the clinical form of IHD, with statistical significance assessed where applicable.

Results. The comorbid profile of women with IHD was dominated by cardiovascular disorders. Hypertension was the most frequently recorded cardiovascular comorbidity, accounting for 34.4%, while heart failure accounted for 14.1%. Other cardiovascular conditions also

contributed to the overall comorbid burden. Chronic IHD accounted for 74.8% of recorded cardiovascular comorbidity, compared with 25.2% in acute IHD, and this difference was statistically significant ($p<0.001$). In the subgroup of married reproductive-age women with IHD, chronic noncommunicable comorbidity was most often represented by anemia (66.2%), followed by type 2 diabetes mellitus (18.0%) and chronic kidney disease (10.8%). In this subgroup, chronic noncommunicable comorbid pathology was identified in 139 cases, and 89.9% of these cases were associated with chronic IHD. Analysis of treatment patterns showed a clear predominance of pharmacological therapy, which accounted for 63.9% of treatment approaches. Non-pharmacological measures accounted for 34.6%, whereas surgical treatment represented 1.5%. Surgical treatment was used more frequently in acute IHD than in chronic IHD. The observed combination of IHD with hypertension, type 2 diabetes mellitus, chronic kidney disease and anemia creates a clinically important background for increased medication burden and requires careful selection and monitoring of pharmacotherapy.

Conclusion. Reproductive-age women with IHD demonstrate a complex comorbid profile in which cardiovascular disease and chronic noncommunicable disorders frequently coexist. Hypertension is the leading cardiovascular comorbidity, while anemia is the most common chronic noncommunicable condition in the analyzed subgroup. The predominance of pharmacological treatment against a background of multiple concomitant diseases supports a personalized approach to drug selection, regular assessment of medication burden, prevention of potentially inappropriate polypharmacy, and systematic pharmacological monitoring. Consideration of the comorbid profile should therefore be an integral component of treatment planning for reproductive-age women with IHD.

Key words: ischemic heart disease; reproductive-age women; comorbidity; pharmacotherapy; polypharmacy; pharmacological monitoring

D. Muzapparova[1], L. A. Dildabekova[1]

ARTIFICIAL INTELLIGENCE IN THE DIAGNOSIS AND TREATMENT OF CHILDREN: FROM CHEMICAL ANALYSIS TO PERSONALIZED MEDICINE

[1]«South Kazakhstan Medical Academy» JSC (Republic of Kazakhstan, Shymkent c., Al-Farabi Square, 1; e-mail: info@skma.kz)

Introduction. The rapid development of artificial intelligence (AI) is creating new opportunities for medical diagnosis, clinical decision support and personalized care. Pediatrics is a particularly important field for these technologies because physiological and biochemical parameters change considerably with age, while clinical symptoms may be nonspecific. Laboratory medicine provides a large amount of quantitative information, including concentrations of glucose, electrolytes, bilirubin, enzymes, hormones, inflammatory markers and other metabolites. Correct interpretation of these data requires consideration of the child's age, biological variability and clinical context. AI can assist clinicians by integrating heterogeneous information and identifying patterns that may be difficult to recognize through manual assessment alone.

Aim. To review the potential role of AI in pediatric diagnosis and treatment, with particular attention to chemical and biochemical laboratory data and the principles of personalized medicine.

Materials and methods. A narrative analytical review was performed using current scientific and medical literature on artificial intelligence in healthcare, pediatric diagnostics, laboratory medicine, clinical biochemistry and personalized medicine. The analysis focused on machine-learning and deep-learning approaches that can process structured laboratory results together with clinical information. Particular attention was given to applications in early detection of disease, risk stratification, interpretation of biochemical profiles and selection of individualized therapeutic

strategies. The potential benefits and limitations of AI were considered from the perspective of safe clinical use. The review did not involve experiments on patients or collection of new biological samples.

Results. The analysis demonstrates that AI can connect chemical and clinical information into an integrated diagnostic profile. In pediatric practice, algorithms may evaluate combinations of laboratory indicators rather than interpreting each result separately. For example, simultaneous assessment of glucose, electrolytes, renal markers and acid-base parameters may support recognition of metabolic disturbances, while combinations of bilirubin and liver-associated enzymes may help characterize patterns of hepatic dysfunction. AI-based systems can also compare a patient's current laboratory profile with previous measurements and detect clinically relevant changes over time. Such tools may support early identification of patients who require additional examination and help clinicians prioritize attention when large numbers of laboratory results are available. The chemical component is especially important because laboratory indicators reflect molecular and metabolic processes occurring in the body. Concentrations of ions, substrates, proteins, enzymes and metabolites can change because of disease, nutrition, growth, medication or physiological adaptation. AI models can learn relationships among these variables and combine them with age, symptoms, vital signs and medical history. This creates a basis for more individualized interpretation instead of applying identical thresholds to all patients. In treatment planning, predictive models may potentially support dose adjustment, monitoring of treatment response and identification of patients at increased risk of adverse outcomes. However, AI should function as a decision-support technology rather than an autonomous replacement for a pediatrician. Model accuracy depends on the quality, completeness and representativeness of training data. Age-related differences, rare diseases, missing laboratory values and differences between medical institutions can affect model performance. Therefore, clinical validation, transparency, protection of patient data and continuous monitoring are essential before implementation in routine pediatric practice.

Conclusion. Artificial intelligence provides a promising connection between chemistry, laboratory diagnostics, medicine and pediatrics. By integrating biochemical measurements with clinical information, AI may improve the interpretation of complex data, support earlier detection of pathological changes and contribute to individualized patient management. The greatest practical value is expected when AI is integrated into the workflow of healthcare professionals and used together with clinical examination and evidence-based medical knowledge. Further research should focus on validated pediatric datasets, explainable algorithms, data security and prospective clinical studies that evaluate real-world effectiveness and safety.

Key words: artificial intelligence; pediatrics; clinical biochemistry; laboratory diagnostics; personalized medicine; machine learning

M. N. Myrzakhanova[1]

CURRENT ADVANCES IN VIRTUAL AUTOPSY USING INTEGRATED VISUALIZATION TECHNOLOGIES

[1]NC JSC «Kokshetau University named after Sh. Ualikhanov» (020000, Republic of Kazakhstan, Kokshetau c., Abay str., 76; e-mail: mmarzhan269@gmail.com)

Introduction. The rapid integration of advanced imaging modalities into clinical and forensic medicine has profoundly transformed contemporary postmortem diagnostics. Traditional invasive autopsy, while historically serving as the gold standard for determining cause of death, inherently carries procedural limitations, biohazard risks, and structural tissue disruption that can obscure subtle pathological changes. Consequently, modern biomedical science increasingly explores non-invasive or minimally invasive alternatives capable of capturing high-fidelity morphological data without

compromising anatomical integrity. Virtual autopsy, commonly known as virtopsy, bridges this diagnostic gap by deploying sophisticated digital imaging protocols. Despite it is growing recognition globally, evaluating the precise diagnostic efficacy of virtopsy – specifically within high-intensity critical care settings – remains an evolving field requiring rigorous prospective validation. Therefore, establishing comprehensive criteria for the application of advanced visualization tools in postmortem examinations represents an urgent scientific objective in modern forensic pathology and clinical practice.

Materials and methods. This investigation was structured as a comprehensive prospective clinical study designed to evaluate the diagnostic utility of virtual autopsy as a reliable counterpart to conventional postmortem examinations. The research cohort comprised critical care patients undergoing management within specialized anesthesiology and intensive care units. To achieve high-resolution digital data acquisition, a multi-modality approach was utilized, incorporating multidetector computed tomography (MDCT), magnetic resonance imaging (MRI), and advanced three-dimensional (3D) digital image reconstruction algorithms. All imaging procedures, subsequent data post-processing, and multi-planar reconstructions were conducted under the strict supervision of certified medical imaging and forensic specialists. Furthermore, exhaustive histological assessments were systematically executed to cross-verify radiological observations. The diagnostic datasets acquired via this non-invasive virtual protocol were subsequently subjected to rigorous comparative analysis against initial clinical diagnoses established during life, as well as the definitive findings obtained through traditional forensic autopsy protocols. This methodology enabled a multi-dimensional appraisal of diagnostic concordance, sensitivity, and the capacity to identify occult lesions.

Results. The analytical evaluation of the prospective data revealed exceptional diagnostic performance, demonstrating that virtual autopsy successfully confirms 88% of preliminary clinical diagnoses established in critical care settings. Beyond high concordance with established clinical records, the deployment of integrated visualization technologies demonstrated a superior capability to detect critical secondary pathologies and acute structural lesions – such as acute hemorrhages, ischemic strokes, and localized pneumothorax – that occasionally evade detection during conventional autopsy due to postmortem tissue alterations or anatomical constraints. The integration of MDCT, MRI, and 3D modeling facilitated precise localization of complex lesions, thereby significantly refining the accuracy of postmortem assessments. These empirical outcomes clearly substantiate the high diagnostic efficacy of virtopsy, highlighting its immense practical value in elevating the overall precision of mortality tracking and expanding diagnostic horizons across both forensic pathology and clinical medicine. Ultimately, the findings underscore the robust potential of virtual autopsy to function as an advanced, reliable non-invasive diagnostic instrument in contemporary healthcare infrastructures.

Conclusion. The conducted study definitively confirms the feasibility and high scientific validity of implementing virtual autopsy as an exceptionally effective complement to, and a viable temporary replacement for, traditional invasive autopsy procedures. By harnessing advanced multidetector computed tomography, magnetic resonance imaging, and three-dimensional reconstruction techniques, the proposed methodology successfully bridges clinical diagnostics and forensic requirements. This innovative diagnostic framework significantly contributes to the systematic modernization of postmortem examination standards, enhances the overall quality and evidentiary reliability of medical-legal evaluations, and opens new avenues for clinical audit and educational advancement in both forensic science and hospital-based clinical practice.

Key words: virtual autopsy; virtopsy; forensic examination; imaging technologies; computed tomography; non-invasive autopsy

A. A. Nikandrova[1, 2], E. S. Komarova[2], D. A. Lukianov[1, 2], Y. V. Zakalyukina[2], V. A. Alferova[2, 3], A. P. Chernyshova[2, 3], M. V. Biryukov[2, 4], P. V. Sergiev[1, 2]

SCREENING AND GENOMIC ANALYSIS OF ANTIBIOTIC-PRODUCING STREPTOMYCES AND CHARACTERIZATION OF ANTIBACTERIAL MECHANISMS

[1]Center for Molecular and Cellular Biology (121205, Russian Federation, Moscow c., Bolshoy Boulevard, 30, building 1; email: arinanikandrova@mail.ru)
[2]Lomonosov Moscow State University (119991, Russian Federation, Moscow c., Leninskie Gory, 1; email: inbox@skoltech.ru)
[3]Shemyakin-Ovchinnikov Institute of Bioorganic Chemistry of the Russian Academy of Science (117997, Russian Federation, Moscow c., Miklukho-Maklaya str., 16/10; email: office@ibch.ru)
[4]Scientific Center for Translational Medicine, Sirius University of Science and Technology (354340, Russian Federation, Sirius Federal Territory, Olympic ave.; email: info@siriusuniversity.ru)

Introduction. Antibiotic resistance remains a major problem and creates a need for new antibacterial compounds and a better understanding of their mechanisms of action. Actinobacteria, especially *Streptomyces*, are an important source of natural antibiotics. Strains isolated from poorly studied habitats may produce bioactive compounds that are useful for further antibiotic research. The aim of this work was to characterize antibiotic-producing *Streptomyces* strains and identify their active compounds, with further study of their mechanisms of action and resistance.

Materials and methods. Two *Streptomyces* strains, BP-8^T and AP22, isolated from different soil samples were studied. Their genomes were sequenced and analyzed to determine their taxonomic position and identify biosynthetic gene clusters. Antibacterial activity was tested using the *E. coli* ΔtolC pDualrep2 reporter system, which allows preliminary classification of antibacterial compounds as inhibitors of protein synthesis or inducers of the DNA damage response. Active compounds were isolated from culture broth by solid-phase extraction and further purification and were analyzed by high-resolution mass spectrometry. For pentalenolactone, resistant *E. coli* clones were selected and sequenced to identify mutations associated with resistance.

Results. Strain BP-8^T was isolated from bamboo rhizospheric soil. Phenotypic, phylogenetic and whole-genome analyses showed that strain BP-8^T represents a new species of the genus *Streptomyces*, which we named *Streptomyces sirii*. The pDualrep2 reporter assay showed that the active compound produced by BP-8^T affects bacterial protein synthesis. The active fraction was purified and the compound was identified as amicetin, a nucleoside antibiotic that inhibits translation. Genome analysis revealed an amicetin biosynthetic gene cluster, supporting the chemical identification of the compound. Several other secondary metabolite gene clusters were also found in the BP-8^T genome. Strain *Streptomyces* sp. AP22 was isolated from soil collected in the Akhshtyr Gorge. Its active compound was purified and identified as pentalenolactone. Pentalenolactone inhibits glyceraldehyde-3-phosphate dehydrogenase (GAPDH), an enzyme involved in glycolysis. Genome analysis of AP22 revealed a pentalenolactone biosynthetic gene cluster. To study resistance to this compound, pentalenolactone-resistant *E. coli* clones were selected. The resistant clones showed an eight-fold increase in the minimum inhibitory concentration compared with the parental strain. Genome sequencing identified a mutation in *gapA* that resulted in a T175S substitution in GapA. To verify that this mutation was responsible for resistance we constructed plasmids carrying either the wild-type *gapA* or the mutant *gapA* T175S and compared the resistance of the transformed cells to pentalenolactone. Expression of the *gapA* mutant variant resulted in a 64-fold increase in resistance compared with the wild-type *gapA*. We proposed using this resistant *gapA* variant as a pentalenolactone-based selectable marker,

providing an alternative to commonly used in molecular biology and medical research antibiotic resistance markers.

Conclusion. In this work, two antibiotic-producing *Streptomyces* strains were characterized and their active compounds were identified. Combining microbiological screening with genome analysis allowed us to identify the produced antibiotics and study their mechanisms of action and resistance. In addition, the T175S substitution in GapA was used to develop a new selectable marker based on resistance to pentalenolactone.

Key words: *Streptomyce*; antibiotic discovery; amicetin; pentalenolactone; mechanisms of action; antibiotic resistance

D. B. Okassov[1], S. A. Ivasenko[1], P. Seité[2], B. Vannier[2], A. B. Marchenko[1]

ANTITUMOR ACTIVITY OF *THYMUS SERPYLLUM* L. EXTRACTS AND THEIR POLYPHENOLIC PROFILES

[1]«Karaganda Medical University named after P. Pospelov» NC JSC (100008, Republic of Kazakhstan, Karaganda, Gogolya st., 40; e-mail: info@qmu.kz)
[2]University of Poitiers (1 rue Georges Bonnet-TSA 51106, 86073, Poitiers Cedex 9, France)

Introduction. Prostate cancer (PCa) is one of the most common malignant diseases in men. More than 550,000 new cases of PCa are reported worldwide each year. Therefore, increasing attention is being paid, both internationally and in Kazakhstan, to the diagnosis, treatment, and prevention of this disease. Given the substantial economic costs associated with the treatment of this disease, as well as the disability burden among men, increasing attention is likewise being paid, both internationally and in Kazakhstan, to its diagnosis, treatment, and prevention. The use of phytotherapy for the treatment and prevention of PCa is also being considered. The aim of this study was to investigate the phenolic composition and antitumor activity of extracts of the medicinal plant *Thymus serpyllum* L., growing in Central Kazakhstan, against the human prostate cancer cell line PC-3.

Materials and methods. The herb of *Thymus serpyllum* was collected in the wild in Central Kazakhstan at the full flowering stage. Three extraction methods were used to obtain the total phenolic compounds from the plant material: heat-assisted extraction, remaceration, and ultrasound-assisted extraction. The extraction solvents were 96% ethanol (96% EtOH), 70% ethanol (70% EtOH), and distilled water. The polyphenolic composition of the extracts was studied using LC-UV-MS. The cell lines were obtained from the American Type Culture Collection (ATCC): the human prostate adenocarcinoma PC-3 cell line (CCL-247) was derived from a grade IV prostate adenocarcinoma of a 62-year-old man, and the RWPE cell line was histologically derived from normal prostate cells of a 54-year-old man. The cytotoxic effects of the obtained *Thymus serpyllum* extracts against the human prostate cancer cell line PC-3 and normal human prostate RWPE cells were investigated in vitro using the colorimetric MTS method with the CellTiter 96® AQueous One Solution Reagent (Promega, USA), according to the manufacturer's protocol.

Results. Depending on the extraction method and solvent selected, statistically significant differences were found in the extraction yields from the studied plant material. Six samples of dry *Thymus serpyllum* extracts were obtained, with yields ranging from 4.30% to 22.4% on an air-dry raw material basis. LC-UV-MS analysis revealed similarity in the qualitative composition of the identified phenolic compounds in the 96% ethanol extracts TS-T96 and TS-US96, the 70% ethanol extracts TS-T70 and TS-US70, and the aqueous extracts TS-RW and TS-USW, irrespective of the extraction method. At the same time, substantial differences were found in the quantitative content

of phenolic acids and flavonoids in the obtained extracts depending on the extraction method and solvent used. The total contents of flavonoids, phenolic acids, and phenolic compounds, as well as the contents of the major components luteolin-7-O-glucoside, apigenin-7-O-glucuronide, and rosmarinic acid, increased in the following order: TS-T96 < TS-T70 < TS-RW and TS-US96 < TS-US70 < TS-USW. According to the MTS assay results, all obtained *Thymus serpyllum* extracts exhibited cytotoxic activity against the human prostate cancer cell line PC-3 and showed a dose-dependent effect. The 96% ethanol extracts (TS-T96, TS-US96) and 70% ethanol extracts (TS-T70, TS-US70), irrespective of the extraction method, showed relatively low cytotoxicity, with IC_{50} values ranging from 280.43 to 345.01 µg/mL (IC_{50} > 200 µg/mL). A relatively high cytotoxic effect against the PC-3 human prostate cancer cell line was observed for the dry aqueous extract of *Thymus serpyllum*, obtained by remaceration, TS-RW, with an IC_{50} = 170.43 µg/mL. It was experimentally established that the dry aqueous extracts TS-RW and TS-USW did not affect the viability of normal human prostate RWPE cells.

Conclusion. The dry aqueous extract of *Thymus serpyllum* L., growing in Central Kazakhstan, exhibited antitumor activity against human PC-3 prostate cancer cells, with an IC_{50}=170.43 µg/mL, while not affecting the viability of normal cells. Therefore, it may be considered a promising pharmaceutical substance for the development of new plant-derived medicinal products for the treatment and prevention of human prostate cancer.

Key words: *Thymus serpyllum*; extraction; phenolic compounds; PC-3 prostate cancer

A. A. Parshutina[1]

THE EFFECT OF DRESSINGS WITH GRANULATED SORBENT AND CHLORHEXIDINE-DIOXIDINE MIXTURE ON WOUND DEFECTS TREATMENT DURATION IN PATIENTS WITH DIABETIC FOOT SYNDROME AT THE OUTPATIENT STAGE

[1]Moscow City Polyclinic No. 66 of the Department of Health (111672, Russian Federation, Moscow c., Saltykovskaya str., 11b)

Introduction. Diabetes mellitus (DM) is a major public health issue. The number of patients with DM has been steadily rising over the past few decades, and in the 21st century diabetes has reached epidemic proportions. Diabetic foot syndrome (DFS) is one of the most severe complications of DM, as it can lead to lower-limb amputation and disability. Treating wound defects associated with DFS remains a pressing challenge in surgery due to the lack of a standardized approaches to minimize/eliminate wound infectious processes, resulting in an increasing number of amputations.

Aim. To evaluate the impact of a dressing technique using a granular sorbent and a chlorhexidine-dioxidine mixture on the duration of wound healing in patients with DFS in an outpatient setting.

Materials and methods. A single-center prospective cohort study was conducted. The study enrolled 129 patients aged 18 years and older with type 2 diabetes mellitus and DFS presenting with Wagner grade 1–3 foot lesions. Exclusion criteria: wounds associated with critical lower-limb ischemia; foot wounds suspected to be of malignant origin; Wagner grade 4 or 5 foot lesions. The patients were randomly divided into two groups. Group 1 was treated using the proposed method involving a chlorhexidine-dioxidine mixture and a granulated sorbent, while Group 2 received treatment with antiseptic dressings containing iodophor solutions. The groups were comparable in terms of baseline characteristics, specifically age, gender, duration of confirmed diabetes and lower-limb atherosclerosis, glycated hemoglobin levels, leukocyte and platelet

counts, and levels of C-reactive protein, erythrocyte sedimentation rate (ESR) and cholesterol. Furthermore, the groups were comparable regarding wound dimensions (area, length, and width) and the calculated ratio: wound length/ wound width.

Results. The results are presented as Me [Q1; Q3]. The duration of treatment was 16 [12–19.25] weeks in the first group and 18 [16–22] weeks in the second group ($p<0.001$). To ensure consistency across the study considering variations in patient wound sizes – a healing rate index was proposed, reflecting the reduction in wound area in square centimeters per week (cm^2/week). To standardize calculations, an additional metric was introduced: wound healing rate relative to the initial wound size (cm^2/week / initial wound area). The healing dynamics of each wound were assessed based on its initial size and individual regeneration rate. The following data were obtained: the median value was 0.06 [0.05–0.08] in the first group and 0.06 [0.05–0.06] in the second group. The differences between the groups were statistically significant: Uemp=1275 vs. Ucrit=1663 ($\alpha=0.05$), $p<0.001$. A comparison of interquartile ranges revealed a significantly higher regeneration rate in the group treated with dressings containing a granular sorbent and a chlorhexidine-dioxidine mixture.

Conclusion. The study demonstrated a statistically significant impact of the dressing technique on duration of outpatient treatment for DFS wounds. The proposed method is suitable for use in outpatient clinics facing time and staffing constraints. The technique is simple to perform, cost-effective, and applicable in various settings, including outpatient surgical offices, rural health posts, hospital surgical and endocrinology departments, and purulent surgery units. According to the self-sterilizing properties of the chlorhexidine-dioxidine solution combination, these dressings can be applied in home settings for patients with limited mobility, as well as during emergency situations or in locations remote from medical facilities. The combined use of the granular sorbent and chlorhexidine-dioxidine mixture accelerates wound healing and reduces the duration of outpatient treatment for DFS patients by two weeks.

Key words: diabetic foot syndrome; diabetes mellitus; dressings; wound process; ulcerative lesion of feet

A. Sabyrbekova[1], A. Worth[2], B. Faizov[1], E. Tulchinsky[1], M. Kriajevskaia[1]

BLADDER CANCER ORGANOIDS AS A PLATFORM FOR TRANSCRIPTOMIC ANALYSIS OF TUMOR DEVELOPMENT AND TREATMENT RESPONSE

[1]Nazarbayev University School of Medicine (Republic of Kazakhstan, Astana c., Kerey and Zhanibek Khandar str., 5/1; e-mail: nusom@nu.edu.kz)
[2]School of Medicine, Deakin University (Australia, Geelong c., Chandos str., 33, Level 6; e-mail: enquiries@dermatologyaustralasia.com.au)

Introduction. Bladder cancer is one of the most common malignancies worldwide, and a substantial proportion of patients present with or progress to muscle-invasive disease. Cisplatin-based chemotherapy is a standard option for these patients, but responses are heterogeneous and acquired or intrinsic chemoresistance frequently limits survival benefit. Chemoresistance therefore remains a major obstacle in the treatment of bladder cancer, and identifying clinically relevant therapeutic targets requires a deeper understanding of the molecular programs that drive tumor development and shape treatment response. The TAM family of receptor tyrosine kinases (TYRO3, AXL, and MERTK), activated by the ligands GAS6 and PROS1, has been implicated in tumor cell survival, migration, immune evasion, and resistance to therapy in several cancer types, which makes these receptors attractive candidates for investigation in bladder cancer.

Conventional two-dimensional cell lines, however, lose much of the cellular heterogeneity and three-dimensional architecture of the original tumor. Three-dimensional organoids preserve key features of the original tumor and provide a physiologically relevant platform for studying tumor biology and drug responses. Combining organoid models with transcriptomic profiling offers a powerful strategy for uncovering the molecular alterations associated with bladder cancer and therapy resistance.

Aim. To establish and characterize a panel of bladder cancer organoid models derived from human and mouse tissue, to evaluate how chemotherapy and AXL-targeted treatment affect these models, with particular attention to the expression of TAM receptors, and to use RNA sequencing to define their transcriptional profiles and identify biological pathways associated with tumor development and treatment response.

Materials and methods. Patient-derived bladder cancer organoids were generated from human tumor tissue and propagated through serial passages to assess their long-term stability. In parallel, mouse organoid models were established from three sources: normal bladder tissue, the MB49 syngeneic tumor model, and tumors induced by the carcinogen N-butyl-N-(4-hydroxybutyl)nitrosamine (BBN). The models were characterized at the tissue and cellular level by immunohistochemistry and immunofluorescence, and at the molecular level by quantitative PCR and Western blotting. Patient-derived organoids were treated with the chemotherapeutic agents cisplatin or gemcitabine, or with an AXL-targeting compound, and changes in morphology as well as in gene and protein expression were evaluated, including expression of TAM receptors and their isoforms. Selected organoid models were subjected to RNA sequencing to identify differentially expressed genes and enriched biological pathways.

Results. Patient-derived organoids were successfully established and stably maintained across multiple passages, supporting their use for longitudinal studies of treatment response. Mouse organoid models were derived from normal and carcinogen-induced bladder tissue, providing complementary systems for comparing normal and tumor phenotypes. Tumor-derived organoids expressed TYRO3, AXL, and MERTK. Chemotherapy altered the expression of specific TAM receptor isoforms, indicating that treatment can reshape receptor expression in bladder cancer cells. RNA sequencing datasets were generated for selected organoid models, and analysis of differentially expressed genes and pathway enrichment is under way to define the transcriptional features of the tumor-derived phenotype and to relate them to treatment response.

Conclusion: Bladder cancer organoids can be established from both patient and mouse tissue and serve as a stable, versatile platform for studying treatment response. The finding that chemotherapy modulates TAM receptor isoform expression supports further investigation of this receptor family as a mediator of chemoresistance in bladder cancer. Integrating these models with transcriptomic analysis provides a framework for identifying molecular signatures and pathways linked to tumor development and chemoresistance. Further integration of transcriptomic findings with functional validation and molecular characterization may help identify candidate therapeutic targets and improve our understanding of treatment response in bladder cancer.Further integration of transcriptomic findings with functional validation and molecular characterization may help identify candidate therapeutic targets and improve our understanding of treatment response in bladder cancer.

Key words: urinary bladder neoplasms; organoids; transcriptomics; RNA sequencing; bioinformatics; treatment response

S. O. Sagadinov[1], A. A. Kazbekova[1], S. V. Yegorov[1]

CONSERVATION OF SURFACE PROTEIN TARGETS FOR STRUCTURE-GUIDED DRUG DEVELOPMENT IN CLINICAL ISOLATES FROM KAZAKHSTAN

[1]Department of Biological and Biomedical Sciences, Nazarbayev University School of Medicine (010000, Republic of Kazakhstan, Astana c., Kabanbay Batyr ave., 53; e-mail: sergey.yegorov@nu.edu.kz)

Introduction. New approaches to treating drug-resistant bacterial infections, including antibodies, nanobodies, computationally designed binders, and vaccines often target specific proteins on the bacterial surface. These molecules are typically designed using reference protein sequences and crystal structures from international databases. But bacteria vary. If clinical strains in a particular region carry different versions of the target protein, a therapeutic designed against the reference may not work locally. We asked a simple question: do the main drug development targets in pneumonia-causing bacteria from Kazakhstan match the reference sequences that researchers worldwide use for drug design?

Materials and methods. We selected 18 surface proteins across three priority drug-resistant pathogens: *Klebsiella pneumoniae* (OmpA, MrkA, MrkD, FimH, FepA, OmpK36), *Acinetobacter baumannii* (OmpA, CsuA/B, BamA, Omp33-36, Bap, FhaB), and *Pseudomonas aeruginosa* (PcrV, OprF, OprI, FliC, PilA, PopB). These proteins play roles in adhesion, biofilm formation, membrane integrity, nutrient uptake, and toxin delivery. We used whole-genome sequencing data from 48 cultured bacterial isolates from pneumonia patients hospitalized in Karaganda, Kazakhstan. Each target was searched against the sequenced genomes using TBLASTN, and the detected sequences were compared to reference proteins by amino acid identity and coverage.

Results. Most targets were highly conserved. When detected, *K. pneumoniae* OmpA and FepA showed 100% and 99.2% median identity to references across 24 samples each. MrkA, FimH, and OmpK36 were similarly conserved in the samples where they appeared. *A. baumannii* OmpA, CsuA/B, and Omp33-36 were each detected in nine samples with 99–100% median identity. *P. aeruginosa* PcrV, OprF, OprI, and PopB were detected in eight to nine samples at 99–100% identity. Two targets stood out as exceptions. PilA, the type IV pilin of *P. aeruginosa*, showed only 37-44% identity to the standard PAO1 reference despite high coverage, indicating that our isolates carry fundamentally different pilin variants. When compared against alternative PilA sequences, identity rose to 90-100%, confirming reference-dependent diversity rather than gene absence. Bap, a large biofilm-associated protein of *A. baumannii*, was not detected in any sample. A subset of *Klebsiella*-associated samples showed lower identity (80–85%) across multiple targets, suggesting divergent lineages or related species requiring further classification. Several samples carried targets from multiple species, consistent with polymicrobial infections common in hospitalized pneumonia patients.

Conclusions. The majority of established drug development targets in our Kazakhstani pneumonia isolates closely match international reference sequences. This supports the use of existing structural data for designing targeted therapeutics against locally circulating strains. However, PilA illustrates that some surface proteins are too variable for single-reference approaches, and divergent bacterial lineages within the cohort highlight the importance of local genomic surveillance. This conservation map across 18 targets and three critical pathogens provides a practical resource for guiding therapeutic and diagnostic development relevant to Central Asian AMR.

Key words: antimicrobial resistance; pneumonia; whole-genome sequencing; surface proteins; drug targets; protein conservation; Kazakhstan

K. S. Satken[1, 2], N. Ablaikhanova[2]

CIRCULATING MIR-20A AS A BIOMARKER FOR EARLY DETECTION OF NON-SMALL CELL LUNG CANCER

[1]Al-Farabi Kazakh National University (050040, Republic of Kazakhstan, Almaty c., Al-Farabi ave., 71; e-mail: info@kaznu.edu.kz)
[2]M. A. Aitkhozhin Institute of Molecular Biology and Biochemistry (050012/A05D3F8, Republic of Kazakhstan, Almaty c., Dosmukhamedova str., 86; e-mail: info@imbb.org.kz)

Introduction. In clinical oncology practice, one of the most challenging tasks is the early detection of cancer, in our case, lung cancer. Despite the availability of low-dose computed tomography, which has increased the rate of cancer detection in high-risk groups, it still has limitations in terms of specificity, which in turn requires repeated imaging studies and invasive diagnostic procedures. These circumstances necessitate the search for other minimally invasive disease biomarkers. One of which may be circulating microRNAs, as they have a stable concentration in the blood and effectively reflect the molecular changes associated with tumor development. miR-20a-5p, a component of the miR-17-92 cluster, is directly linked to signaling pathways involved in cell proliferation, apoptosis, and cell migration, changes in which contribute to the emergence and development of a tumor. The aim of this review was to determine whether miR-20a has the potential to serve as a diagnostic biomarker for the early detection of NSCLC.

Materials and methods. A descriptive review was conducted of peer-reviewed experimental and diagnostic studies, as well as systematic reviews, devoted to the study of miR-20a in lung cancer. The publications were evaluated taking into account the analyzed biological material, the stage of the disease, the analytical platform, the normalization method, and the composition of the diagnostic model. Since the focus is on assessing a biomarker for early diagnosis, considerable emphasis was placed on studies involving patients at an early stage, in which the independent use of miR-20a or its combined use as a biomarker was considered. In addition, sensitivity and specificity indicators were taken into account, as well as the area under the ROC curve (AUC). Preanalytical and analytical sources of variability were also considered, including hemolysis, contamination of samples with blood cells, sample processing conditions, RNA extraction, and the selection of reference controls.

Results. The available data indicate a direct role of miR-20a in the molecular biology of NSCLC. Studies confirm the impact of changes in miR-20a expression on the transcription factors of the E2F family and on the regulation of such targets as PTEN, ferroportin, and EGR2. Such interactions may contribute to the progression of the cell cycle, increase the survival and invasive potential of tumor cells, and also participate in the development of therapy resistance. Studies indicate that the level of circulating miR-20a makes it possible to distinguish patients with NSCLC at an early stage of the disease from all others cancer-free individuals. In the study, miR-20a, together with miR-145, miR-21, and miR-223, yields an AUC of 0.897, with a sensitivity of 81.8% and a specificity of 90.1%. Another study, when using miR-20a individually in blood plasma, showed an AUC value of 0.89, which indicates that the inclusion of additional microRNAs increases the accuracy of detecting lung cancer. However, data on the nature of changes in miR-20a levels in various studies are contradictory. Elevated concentrations were observed mainly in plasma, whereas a number of studies of blood serum in patients with resectable tumors or stage I–II disease revealed a decrease in miR-20a-5p expression. Despite these discrepancies, in the course of systematic assessments of biomarkers for early-stage lung

cancer, miR-20a retains its status as a promising circulating marker that provides clinically significant differential diagnosis. The observed differences may be due to variations in the biological material (plasma or serum), the stage of the tumor process, the histological type of the tumor, patient characteristics, as well as methodological factors: hemolysis control, data normalization strategy, and the design of the analytical test system. The results obtained indicate that miR-20a carries important diagnostic information, but its interpretation largely depends on the conditions under which the samples are collected and analyzed.

Conclusion. Circulating miR-20a is a promising biomarker for the early detection of NSCLC. The greatest value of this marker likely lies not in its independent use, but in its inclusion in a panel of several microRNAs, combined with an assessment of clinical risk factors and imaging data. To implement this approach in clinical practice, prospective multicenter studies are needed to standardize blood collection procedures, plasma or serum preparation, hemolysis assessment, RNA extraction, RT-qPCR data normalization, and the selection of threshold values. Thorough methodological unification is necessary to determine whether testing based on miR-20a can improve the specificity of lung cancer screening and reduce the frequency of unjustified invasive interventions.

Key words: miR-20a; lung cancer; non-small cell lung cancer; early detection; circulating microRNA; liquid biopsy; biomarker

V. N. Shashkova[1], D. S. Tyulegenova[1], A. A. Malvenova[1], B. K. Kurmangazhina[1], Ye. A. Tulebayev[1]

DRUG ENCAPSULATION TECHNOLOGY

[1]M. Kozybayev North Kazakhstan university (150000, Republic of Kazakhstan, Petropavlovsk c., Pushkin str., 86; e-mail: mail@ku.edu.kz)

Introduction. Drug encapsulation encloses an active substance within a carrier or distributes it throughout a polymer matrix. It supports development of dosage forms with modified release and reproducible quality. Alginate systems provide a model for examining how composition and processing influence drug retention and release. Performance depends on the active substance and carrier structure; particle formation alone does not establish therapeutic benefit. Aim: to identify factors affecting alginate-based drug encapsulation and priorities for formulation optimization and quality assessment.

Materials and methods. A narrative analysis of four published experimental studies was supplemented by a review of probiotic encapsulation and sustainable manufacturing principles. The studies investigated alginate carriers containing adsorbents, antibiotics, probiotics, vitamins, thick herbal extracts, macro- and microelements, and model compounds with different solubilities. Dripping with ionic crosslinking, modified emulsification, and spray-coagulation were examined. Data were compared qualitatively for polymer and calcium chloride concentrations, droplet formation, hardening, particle characteristics, encapsulation efficiency, and in vitro release. The analysis distinguished drug retention from loading and assessed whether optimization addressed several quality attributes. No pooled effect estimate was calculated because active substances, preparation procedures, and release conditions differed.

Results. Encapsulation performance was formulation-specific. In the ibuprofen study, factorial design identified effects of sodium alginate, calcium chloride, and magnesium stearate on formulation performance. The findings support evaluating interacting formulation variables. In the metformin hydrochloride study, polymer concentration, drug loading, crosslinker concentration,

and crosslinking time were investigated; microspheres sustained drug release for eight hours under the reported in vitro conditions. This result cannot be transferred directly to another active substance. In the doxorubicin study, collection distance, hardening time, and calcium chloride concentration affected spherical integrity. The formulation optimized for integrity had encapsulation efficiency of 40.62% and drug loading of 3.52%. Another formulation retained more drug but showed poorer release, indicating that maximum encapsulation efficiency does not necessarily identify the most suitable carrier. Drying produced shrinkage and surface cracks; changes in release medium altered the release profile. The spray-coagulation study produced porous alginate microparticles and examined loading and release of model compounds with different solubilities. Delayed release of the poorly water-soluble compound in acidic conditions emphasized the importance of drug properties and medium selection. Priorities include particle size and morphology, drug content, encapsulation efficiency, loading, and release kinetics. Encapsulation efficiency describes the fraction of initially introduced drug retained in the carrier; loading describes the drug fraction within recovered particles. Neither measure is equivalent to total particle yield. Our review examined extrusion, spray drying, freeze drying, emulsification, and hydrogel-based encapsulation of *Lactiplantibacillus plantarum* in synbiotic formulations to protect probiotic viability during processing, storage, and gastrointestinal transit. Microcapsules of varied compositions have been produced containing activated charcoal, metronidazole, probiotic cultures, vitamin E, a thick extract of *Filipendula ulmaria* (meadowsweet) herb, and macro- and microelements; prototypes underwent preliminary assessment of quality and *in vitro* biological activity. Green encapsulation technology aligns with Sustainable Development Goal (SDG) 3 through pharmaceutical quality and safe delivery, SDG 9 through process innovation, and SDG 12 through resource efficiency and waste prevention. Aqueous processing, renewable biodegradable carriers, and reduced hazardous solvent use are development priorities. Lower energy demand may support SDG 13 if emission reductions are verified. These directions require life-cycle assessment of raw materials, water use, drying energy, effluents, and end-of-life impacts to establish environmental advantages.

Conclusion. Alginate-based encapsulation provides a platform for investigating modified drug release, but performance depends on control of formulation and processing. Polymer and crosslinker concentrations should be evaluated with droplet formation, hardening, drying, and release conditions. Formulation selection should balance retention, loading, structural integrity, and intended release. Further development requires reproducibility, stability, and safety assessment; in vitro release alone does not demonstrate improved clinical efficacy. Sustainable process design should support pharmaceutical optimization.

Key words: drug encapsulation; sodium alginate; modified release; green technology; Sustainable development goal; SDG

E. V. Sheyda[1], A. G. Duskaeva[2]

DOSE-DEPENDENT EFFECT OF ZINC ON RAT ACTIVITY AND BEHAVIOR

[1]Federal Research Center for Biological Systems and Agrotechnologies of the Russian Academy of Sciences (460000, Russian Federation, Orenburg c., 9 Yanvarya St., 29; e-mail: elena-shejjda@mail.ru)
[2]Pirogov Russian National Research Medical University (117513, Russian Federation, Moscow c., Ostrovityanova St., 1; e-mail: gduskaev@mail.ru)

Introduction. Maintaining adequate zinc intake is crucial for optimal health. The bioavailability and functional properties of zinc can be influenced by the food matrix or the form of zinc used in a supplement.

Aim. To evaluate the emotional state, locomotor activity, and behavior of laboratory animals (rats) following the administration of zinc aspartate.

Materials and methods. The study investigated the effects of zinc aspartate at doses of 1.7, 3.4, and 5.1 mg/kg on the behavioral activity of Wistar rats using the «Open Field» test, the «Light-Dark Box» test, and an infrared actimeter system. Assessments were conducted on days 1, 7, and 21 of the experiment.

Results. In the «Open Field» test, horizontal locomotor activity (HLA) metrics demonstrated a pronounced dose-dependent response. In Group II animals (1.7 mg/kg), HLA was 21-35% higher than in the control group, indicating a stimulatory effect of the moderate zinc dose. Conversely, Groups I and III showed a decrease in HLA by 8-10% and 7-52%, respectively, particularly at the maximum dose. At the same time, the exploratory component of HLA increased significantly across all experimental groups: 1.73-fold in Group I, 1.29-fold in Group II, and 1.54-fold in Group III (on day 7); this suggests heightened interest in the novel environment, despite the overall suppression of movement. Total HLA was highest in Group II (exceeding control levels) and lowest in Group III, pointing to a potential inhibitory effect of the high zinc dose. Vertical activity (jumping, rearing) decreased in all groups compared to the control on day 7, but a trend toward recovery was observed by day 21, especially in the moderate-dose group. Grooming metrics were highest in Group I: on day 7, they were 2 times higher than in Group II and 9.4 times higher than in Group III; on day 14, they were 1.3 and 4.19 times higher, respectively. This may indicate increased anxiety in animals receiving the medium dose. In Group III, grooming levels hardly differed from the control, suggesting a less pronounced emotional response at the high dose. The number of hole-poking events (a marker of curiosity) exceeded that of the control group (15.6±1.04) only in Group I (17.3±2.28) and remained at this level until day 21, despite a general decline in activity by the end of the experiment. Defecation, an indicator of stress, was minimal in Group II (19.5% and 62.5% lower than the control on days 7 and 21, respectively), which may suggest better adaptation. The highest number of defecation events was recorded in Group I; this aligns with increased grooming behavior and indicates an anxious state. In the light-dark box test, control animals initially explored both chambers actively, but by day 14, they showed less willingness to enter the light zone – a typical pattern during the adaptation process. Zinc administration altered behavior: animals in Group I (3.4 mg/kg) almost completely avoided the light chamber and peered out from the dark chamber five times less frequently than the controls, indicating pronounced anxiety. High activity in the light chamber was observed in Group II (1.7 mg/kg): on day 7, these animals spent 82% more time there than those in Group III. By day 21, the difference between Groups II and III had increased 4.4-fold, suggesting a sustained anxiolytic effect of the moderate dose. Animals in Group III (5.1 mg/kg) exhibited intermediate behavior but still showed a preference for the dark chamber. In the infrared actimeter system, control animals gradually reduced their activity levels by day 21. In Group I (3.4 mg/kg), suppressed movement was noted on days 7 and 14, but activity recovered to control levels by the end of the experiment. In Group II (1.7 mg/kg), persistent suppression of activity was observed throughout the study period. In Group III (5.1 mg/kg), the pattern differed: excitation was observed on days 7 and 21, whereas marked suppression occurred on day 14, which may indicate an unstable neurobehavioral response at the high dose.

Conclusion. Zinc aspartate exerts a dose-dependent effect on rat behavior. A moderate dose (1.7 mg/kg) helps reduce anxiety and maintain exploratory activity. Intermediate (3.4 mg/kg) and, especially, high (5.1 mg/kg) doses induce signs of emotional tension, reduced interest in the environment, and instability in locomotor activity. The most favorable behavioral profile is observed at a dose of 1.7 mg/kg.

Key words: behavior; zinc aspartate; laboratory animals

L. Stabayeva[1], M. Mergazina[1], Ye. Kamyshanskiy[2], Zh. Amirbekova[1]

MYXOID HISTOPHENOTYPE OF THE CERVICAL STROMA AS A POTENTIAL MORPHOLOGICAL MARKER OF HIGH-RISK CIN PROGRESSION

[1]Department of Morphology, «Karaganda Medical University named after P. Pospelov» NC JSC (100008, Republic of Kazakhstan, Karaganda, Gogolya st., 40; e-mail: info@qmu.kz)
[2]Department of Pathology, Clinic of «Karaganda Medical University named after P. Pospelov» NC JSC (100008, Republic of Kazakhstan, Karaganda, Gogolya st., 40; e-mail: info@qmu.kz)

Introduction. Cervical intraepithelial neoplasia (CIN) is a precancerous condition characterized by substantial morphological and biological variability in its clinical course. Early identification of patients at high risk of lesion persistence and progression is of particular importance. Currently, morphological diagnosis focuses primarily on epithelial changes, whereas the cervical stroma and extracellular matrix remain insufficiently studied as potential prognostic indicators. Extracellular matrix remodeling may reflect alterations in the tumor microenvironment accompanying neoplastic transformation.

Aim. To assess the diagnostic and potential prognostic significance of extracellular matrix histophenotyping of the cervical stromal tissue in CIN of varying severity, as well as in cases of persistent and progressive neoplasia.

Materials and methods. A retrospective study was conducted on 160 cervical biopsy and surgical specimens obtained from women of reproductive age with CIN 1–3 and confirmed persistence or progression of the lesion on follow-up examination. The control group consisted of 40 specimens of morphologically intact cervical tissue. Histological and histochemical evaluation was performed using hematoxylin and eosin staining and Masson's trichrome staining. Based on the condition of the stromal collagen framework, three histophenotypes were identified: normal, intermediate, and myxoid.

Results. A statistically significant difference in the distribution of stromal histophenotypes was observed according to the severity of CIN ($p<0.001$). The normal histophenotype, characterized by organized parallel bundles of type I collagen, was identified in 97.5% of control specimens, 27.5% of CIN 1 specimens, and 12.5% of CIN 2 specimens, and was absent in CIN 3. The intermediate histophenotype predominated in CIN 1 and CIN 2, accounting for 67.5% and 72.5% of cases, respectively. In CIN 3, the myxoid histophenotype became predominant and was identified in 55% of cases. More pronounced stromal remodeling was observed in patients with persistent or progressive CIN. Among the 24 patients with an unfavorable clinical course, the normal histophenotype was identified in 12.5% of cases, the intermediate histophenotype in 25.0%, and the myxoid histophenotype in 62.5%. An association was also identified between the stromal histophenotype and HPV 16/18 infection. These HPV types were detected predominantly in specimens with the intermediate (69.1%) and myxoid (27.2%) histophenotypes and in only 3.7% of cases with the normal histophenotype ($p<0.001$).

Conclusion. The myxoid histophenotype of the cervical stromal extracellular matrix is associated with a high grade of epithelial dysplasia, as well as with persistence and progression of CIN. The observed sequential transformation of the stromal pattern from normal to intermediate and subsequently to myxoid may reflect pathological remodeling of the microenvironment during neoplastic transformation. Stromal histophenotyping may represent a promising additional morphological tool for risk stratification in patients with CIN and could potentially be used to refine follow-up strategies and identify patients requiring closer oncological surveillance. However, prospective multicenter studies and external validation are required to confirm the independent prognostic value of this approach.

Key words: cervical intraepithelial neoplasia; HPV 16/18; cervical stroma; extracellular matrix; myxoid histophenotype; stromal remodeling; progression; precancerous lesion

D. A. Starodubtseva[1], S. A. Panov[2], D. Zh. Danayeva[3]

CHANGES IN OXIDATIVE STRESS AND MITOCHONDRIAL ACTIVITY MARKERS DURING PERSONALIZED METABOLIC CORRECTION: A RETROSPECTIVE CASE SERIES

[1]Nano Identica, BIOIDENTICA LLP (050000, Republic of Kazakhstan, Almaty, S. Amanzholova str., 38, office 6; e-mail: darya@mitolab.kz)
[2]Research Institute of Cellular Diagnostics and Mitochondrial Medicine, LMB Clinic, LMB CLINIC LLP (050010, Republic of Kazakhstan, Almaty, Samal-2 microdistrict, 63; e-mail: info@mitolab.kz)
[3]Department of Biophysics, Biomedicine, and Neurobiology, Al-Farabi Kazakh National University (050040, Republic of Kazakhstan, Almaty, 71 Al-Farabi Ave.; e-mail: eekoffee@gmail.com)

Introduction. Disruptions in cellular energy metabolism and the development of oxidative stress are considered important components of metabolic dysfunction. Mitochondria play a central role in cellular bioenergetics, regulation of redox balance, and maintenance of innate immune function, including phagocytosis. When mitochondrial function is impaired, the balance between reactive oxygen species production and antioxidant defence shifts towards oxidative stress, which in turn affects protein synthesis, membrane integrity, and the functional activity of leukocytes. Personalised treatment programmes may include substances that influence antioxidant systems, mitochondrial metabolism, and cellular energy metabolism, including metabolic substrates, cofactors, and micronutrients. However, most published studies evaluate such substances in isolation or in fixed combinations, whereas in real clinical practice they are frequently used together, with the composition and dosage adapted to the individual patient. As a result, the nature of changes in functional cellular parameters when these substances are used in combination, and the extent to which these changes are consistent across patients and over time, remain insufficiently studied.

Materials and methods. A retrospective analysis was conducted of 16 clinical cases with at least two consecutive measurements of cellular functional parameters. The duration of follow-ups ranged from 39 to 183 days. We analyzed phagocytosis, oxygen and energy metabolism (OEM), oxidative stress, protein metabolism, and mitochondrial activity. For each patient, we compared the first and last available time points. The results were considered exploratory due to the individualised nature of the therapeutic programmes.

Results. The median oxidative stress index decreased from 37.5% at the initial examination to 13.5% at the follow-up. A decrease in this index was observed in 12 of 16 patients; the median individual change was – 30 percentage points. The median protein metabolism index increased from 13.5% to 53.5%, with an increase observed in 12 of 16 patients. The median individual change was +28 percentage points. The median mitochondrial activity increased from 4% to 29%. An increase in this index was recorded in 13 of 16 patients, and the median individual change was +17.5 percentage points. For oxygen and energy metabolism, the median was 21% at baseline and 28.5% at the last examination; an increase was recorded in 11 of 16 patients. Phagocytosis indices were characterised by the most pronounced interindividual variability, with both increases and decreases observed, and no consistent direction of change across the group. Analysis of patients with three or more consecutive measurements revealed cases of non-linear dynamics, in which a marked change in the index at an intermediate time point was not sustained during further observation. In several cases, the direction of change differed between individual parameters within the same patient, suggesting that the response to metabolic correction is not uniform across functional domains.

Conclusion. In the analyzed series of clinical cases, personalized metabolic correction was predominantly accompanied by a decrease in oxidative stress indicators and an increase in protein metabolism and mitochondrial activity indicators. At the same time, significant interindividual and temporal variability was observed in a number of cellular indicators. The results obtained indicate the potential value of serial cellular monitoring and justify the conduct of prospective studies with a standardized treatment protocol, predefined endpoints, and a control group.

Key words: oxidative stress; mitochondrial activity; protein metabolism; phagocytosis; oxygen and energy metabolism; personalised metabolic correction

O. E. Tabakchi[1], D. D. Mukhametova, A. Kh. Odintsova[2], D. I. Abdulganieva[1]

ULTRASOUND IMAGING OF SKELETAL MUSCLES IN THE COMPREHENSIVE DIAGNOSIS OF SARCOPENIA IN PATIENTS WITH INFLAMMATORY BOWEL DISEASE

[1]Kazan State Medical University (420012, Russian Federation, Kazan, Butlerova str., 49; e-mail: olya-akchurina@mail.ru)
[2]Republican Clinical Hospital (420064, Russian Federation, Kazan, Orenburgsky tract, 138)

Introduction. Sarcopenia is characterized by progressive and generalized loss of skeletal muscle mass and strength, leading to functional impairment and impaired clinical outcomes. In inflammatory bowel disease (IBD), chronic systemic inflammation, malabsorption, nutrient deficits, and prolonged corticosteroid exposure significantly contribute to secondary alterations in body composition. Early identification of muscular depletion remains essential for timely nutritional and therapeutic optimization; however, standard cross-sectional techniques such as computed tomography (CT) involve ionizing radiation and high costs, making routine screening challenging.

Aim. To evaluate peripheral muscle mass parameters using musculoskeletal ultrasonography and establish its diagnostic performance in identifying sarcopenia among individuals with inflammatory bowel disease.

Materials and methods. A comparative prospective observational study enrolled 136 adult patients with confirmed IBD, comprising 62 (45.6%) individuals with ulcerative colitis and 74 (54.4%) with Crohn's disease. The healthy control group (CG) consisted of 30 matched individuals. Female participants accounted for 47.1% (n=64) of the cohort with IBD and 56.7% (n=17) of the CG. The median age of patients with IBD was 39 [28; 50] years compared to 33 [27.25; 38] years in the CG. Anthropometric assessment included body mass index (BMI), mid-upper arm circumference (MUAC), and mid-thigh circumference (MTC). Muscle strength was quantified via standard handgrip dynamometry against sex- and age-stratified norms. Ultrasound (US) sonography was performed to measure muscle thickness at two predefined anatomical landmarks: the mid-upper arm (US-MA) and mid-thigh (US-MT). The skeletal muscle index (SMI-BIA) was evaluated via multifrequency bioimpedance analysis using the ABC-02 Medass system. In 28 hospitalized patients with IBD who underwent diagnostic abdominal CT at enrollment, the CT-derived skeletal muscle mass index (SMI-CT) at the L3 lumbar vertebra level was calculated, adopting cutoff thresholds for sarcopenia of 36.5 cm^2/m^2 in males and 27.3 cm^2/m^2 in females. Statistical analysis included Mann – Whitney U testing, Spearman rank correlation, and receiver operating characteristic (ROC) analysis.

Results. Stratification by BMI demonstrated normal body weight in 76 (55.8%) patients, underweight in 20 (14.7%), overweight in 30 (22.1%), and obesity in 10 (7.4%). Anthropometric

arm and thigh circumferences did not differ significantly between females with IBD and healthy female controls. Conversely, males with IBD exhibited significantly reduced MUAC (28.55 [25.95; 31.77] cm vs 33.00 [31.80; 34.50] cm, $p < 0.05$) and MTC (48.00 [45.38; 51.32] cm vs 54.00 [54.00; 55.00] cm, $p<0.05$) relative to male controls. Dynapenia was documented in 16.7% of women and 11.6% of men with IBD, whereas low muscle mass by SMI-BIA occurred in 31.8% of patients overall. Sonographic assessment revealed that female patients with IBD had significantly lower US-MA values (19.38 [17.27; 22.35] mm vs 21.58 [20.21; 22.66] mm, $p<0.05$) than healthy female counterparts, while male cohorts demonstrated comparable upper arm thicknesses. Mid-thigh muscle thickness was markedly decreased in both sexes with IBD: females had a median US-MT of 30.84 [23.21; 36.37] mm versus 41.30 [35.79; 43.73] mm in the CG ($p<0.05$), and males showed 30.61 [25.96; 39.26] mm versus 41.53 [39.06; 42.41] mm in the CG ($p<0.05$). Correlation analysis indicated significant positive relationships between US-MA and MUAC ($r=0.535$), BMI ($r=0.434$), SMI-BIA ($r=0.718$), and dynamometry ($r=0.643$, all $p<0.05$). Similarly, US-MT correlated with MTC ($r=0.511$), BMI ($r=0.401$), SMI-BIA ($r=0.334$), and dynamometry ($r=0.221$, all $p<0.05$). Among patients assessed by abdominal CT, 8 individuals (40%) fell below the diagnostic thresholds for sarcopenia. ROC curve analysis identified US-MT as a statistically robust predictor of CT-confirmed sarcopenia, with an area under the curve (AUC) of 0.826 (95% CI: 0.666–0.986, $p=0.009$). The resulting optimal diagnostic model achieved a sensitivity of 75.0% and a specificity of 83.3%.

Conclusion. Conclusion. Musculoskeletal ultrasound assessment of limb muscle thickness, particularly of the mid-thigh, may reflect peripheral skeletal muscle depletion in patients with ulcerative colitis and Crohn's disease. Given its observed correlation with computed tomography and functional dynamometry, muscle ultrasonography could potentially be considered a feasible, safe, non-invasive, and radiation-free complementary screening modality for evaluating sarcopenia risk in patients with inflammatory bowel disease, although further validation in larger cohorts is warranted.

Key words: inflammatory bowel disease; sarcopenia; musculoskeletal ultrasound; muscle thickness; computed tomography; bioelectrical impedance analysis

L. R. Takhauova[1], A. R. Takhauov[1], L. V. Smagliy[1]

PROTEOMIC PROFILING OF TEAR FLUID TO IDENTIFY MOLECULAR SIGNATURES OF CHANGES IN OCULAR SURFACE STATUS

[1]Seversk Biophysical Research Center, Federal Medical and Biological Agency of Russia, Seversk, Russia (636013, Russia, Tomsk Region, Seversk, Chekist Lane, 7, bldg. 2, tahauovaa@gmail.com)

Introduction. The development of high-throughput molecular profiling technologies has significantly expanded the capabilities of modern biomedicine. Proteomics enables the simultaneous characterization of numerous protein components within a biological system, allowing the investigation of not only individual molecules but also interconnected functional processes. Proteomic technologies are particularly valuable for identifying molecular markers of early changes, when clinical manifestations of disease may be absent or nonspecific. The ocular surface represents a promising model for molecular investigations owing to the accessibility of tear fluid as a biological specimen. The tear film is in direct contact with the corneal and conjunctival epithelia and contains a broad spectrum of proteins involved in the regulation of local immune responses, inflammation, cell adhesion, antioxidant defense, and tissue repair processes.

Aim. To perform proteomic profiling of tear fluid and evaluate the potential of this approach for identifying molecular characteristics associated with the functional status of the ocular surface.

Materials and methods. Five tear fluid samples were analyzed. Protein identification was performed using high-performance liquid chromatography coupled with high-resolution tandem mass spectrometry. The analysis was conducted using a nanoLC Dionex Ultimate 3000–Orbitrap Q Exactive HF-X platform.

Results. A total of 837 proteins were identified. Comparative analysis across samples revealed that 229 protein components were detected in all samples, whereas 608 exhibited variability in their detection across the samples. Thus, the tear fluid proteome comprised a relatively stable component alongside a substantial pool of proteins displaying interindividual variability. The observed protein diversity provides an opportunity for functional characterization of the proteome using contemporary bioinformatics approaches. Of particular interest are proteins associated with inflammatory and immune processes, redox homeostasis, maintenance of the epithelial barrier, and intercellular interactions. A major advantage of the proteomic approach is its ability to assess multiple functional systems simultaneously. This makes it possible to interpret changes in protein profiles not merely as isolated alterations in individual molecular markers, but as reflections of coordinated changes in interconnected biological processes. Further research will involve functional annotation of the identified proteins, enrichment analysis of biological processes and molecular pathways, and correlation of proteomic characteristics with clinical parameters of ocular surface status. This approach may facilitate the development of molecular panels potentially suitable for the early characterization of functional abnormalities. Another promising direction is the use of the obtained proteomic profile as a foundation for the subsequent integration of data from different OMICs levels. Integrating proteomic and clinical data with other molecular datasets, where appropriate biological material is available, may enable a transition from descriptive characterization of tear fluid composition to a systems-level analysis of the mechanisms underlying changes in ocular surface status.

Conclusion. High-resolution mass spectrometry-based proteomic profiling of tear fluid represents a promising tool in modern biomedicine for identifying molecular signatures of changes in ocular surface status. The findings provide a foundation for subsequent bioinformatics analyses and the development of approaches for the molecular stratification of functional states.

Key words: tear fluid proteomics; ocular surface; high-resolution mass spectrometry; molecular biomarkers

B. M. Turabayeva[1], M. E. Ospanova[1], T. S. Baltabayeva[1], K. H. Zhangazieva[1], S. A. Abdrakhmanova[1]

PREPARATION OF APHERESIS PRODUCT FOR CAR-T THERAPY: EXPERIENCE OF THE SCIENTIFIC AND PRODUCTION CENTER FOR TRANSFUSIOLOGY

[1]RSE on REM «Scientific and Production Center of Transfusiology» of the MH RK (010000, Republic of Kazakhstan, Astana c., Kerey Zhanibek Khans str., 10; e-mail: omninpct16@mail.ru)

Introduction. CAR-T cell therapy is one of the promising approaches in personalized cellular therapy, particularly for the treatment of hematological malignancies. The efficacy and safety of this technology largely depend on the quality of the starting cellular material obtained through leukapheresis. The apheresis product should contain an adequate number of cells, including CD3+ T lymphocytes, for subsequent isolation, genetic modification, and expansion. In major clinical studies supporting the registration of several CAR-T products, CD3+ cell content was considered an important

characteristic of the starting material; manufacturing protocols for registered products have used a reference level of at least 1×10^9 CD3+ cells. However, this value should not be considered a universal regulatory threshold, as requirements may vary depending on the specific manufacturing platform and protocol. Variability in the cellular composition of the collected product, associated with the baseline characteristics of donors or patients and leukapheresis parameters, makes its comprehensive characterization an important component of quality control.

Aim. According to the FDA approach to the characterization of cellular starting material, key quality parameters include cellularity, cell viability, CD3+ cell content, and microbiological purity. With the implementation of cellular therapy technologies into clinical practice in the RK, there is a need to accumulate local experience in leukapheresis, evaluate the characteristics of collected cellular products, and develop standardized approaches to their quality control.

Materials and methods. The results of 13 leukapheresis procedures performed at the Scientific and Production Center for Transfusiology between November 2024 and June 2026 were analyzed. The study included healthy donors as well as patients with hematological malignancies. Cellular products were collected using the Spectra Optia automated blood cell separator (Terumo BCT, USA) with the Mononuclear Cell Collection protocol. The following parameters were assessed: total blood volume processed, processed total blood volume expressed as the number of total blood volumes (TBV), procedure duration, volume of the collected cellular product, white blood cell (WBC) count, and CD3+ cell count in the collected product. Immunophenotyping of the cellular product was performed by flow cytometry. Microbiological safety was assessed by bacterial sterility testing. Prior to leukapheresis, screening for transfusion-transmissible infections was performed using immunochemiluminescence assay (ICLA) and polymerase chain reaction (PCR).

Results. The volume of the collected cellular product ranged from 60 to 265 mL. The processed blood volume varied from 1.0 to 2.6 total blood volumes, while procedure duration ranged from 136 to 316 minutes. The WBC count in the collected product ranged from 6.5 to 32.1×10^9 cells. The CD3+ cell count in the apheresis product ranged from 1.07×10^9 to 1.63×10^{10} cells per dose. The observed values demonstrate variability in the cellular composition of the collected apheresis products, which may be associated with the baseline characteristics of donors and patients, as well as individual procedural factors. Bacteriological testing of the analyzed samples confirmed the sterility of the cellular products. The results demonstrate the feasibility of obtaining cellular products suitable for subsequent use in the manufacturing process of CAR-T cells. The accumulated experience also provides a basis for further development of standardized approaches to leukapheresis and characterization of cellular starting material.

Conclusion The experience gained demonstrates the readiness of the Scientific and Production Center for Transfusiology to perform one of the key stages of the CAR-T manufacturing process-collection and cellular characterization of the starting material. Further accumulation of data will enable standardization of leukapheresis procedures and identification of factors influencing the cellular composition of the collected product.

Key words: CAR-T therapy; leukapheresis; CD3+ T cells; WBC; transfusion medicine

P. D. Utepov[1]

ORGANIZATION OF A BIOSAFETY SYSTEM FOR LABORATORY PERSONNEL

[1]South Kazakhstan Medical Academy (160000 Republic of Kazakhstan, Shymkent c., Nursat str., 18; e-mail: utepov.parkhat@mail.ru)

Introduction. The healthcare system of every state is aimed at protecting and preserving the health of its population. Scientific and technological advances in biomedicine are actively being

implemented in practical healthcare. At the same time, diagnostic laboratory testing of biological substances from humans and animals, as well as environmental samples, is aimed at identifying microorganisms – the causative agents of diseases - and determining their pathogenic properties and potential danger to humans. Medical laboratory personnel whose activities involve handling pathogenic biological agents (PBAs) belong to a high-risk group. The relevance of this study is determined by the need to analyze the implementation of regulatory acts in the fields of biosafety and biosecurity.

Materials and methods. The methodological basis of the study was dialectics as a general scientific method of cognition. The formal - logical method and content – analysis were also applied to regulatory acts.

Results. The regulatory framework for ensuring biosafety and biosecurity for specific professional groups whose activities involve the handling of PBAs, as well as for the country as a whole, is based on the International Health Regulations (2005), Third Edition, the Laboratory Biosafety Manual, Fourth Edition, and various standards and guidelines recommended by the World Health Organization (WHO). In the Republic of Kazakhstan, the Law «On Biological Safety of the Republic of Kazakhstan» was adopted. Amendments and additions were also introduced to the legislation on the healthcare system and public health, and 13 orders were issued by the authorized healthcare body of the Republic. The principal legislative document regulating the activities of entities, including healthcare organizations, involved in the handling of PBAs is the Law of 21 May 2022 «On Biological Safety of the Republic of Kazakhstan». The law includes five main elements: 1) State control and regulation of activities carried out by state organizations in the field of biosafety, including: mandatory registration of all existing and newly established laboratories and production facilities that handle PBAs hazardous to humans and animals, regardless of their ownership structure or institutional affiliation; licensing of services provided by legal entities and individuals for disinfection, disinsection, and deratization;strengthening of administrative and criminal liability for the illegal handling, sale, and theft of dangerous pathogens, as well as for violations of handling procedures that result in serious consequences. 2) Recording and monitoring of potential biological risks and biological threats. This includes the development and implementation of a unified state information system, «Biosafety», which will consolidate data on the activities of laboratories and production facilities involved in handling PBAs that are hazardous to humans, animals, and plants. 3) Organization of preventive measures in the field of biosafety, including: increasing the readiness of Kazakhstan's infrastructure to counter biological threats through strengthening the material and technical capacity of medical and veterinary institutions, including their laboratories, as well as through the construction of new pharmaceutical production facilities; coordination and management of operational response teams dealing with biological incidents and epidemiological and veterinary emergencies. 4) Human resources. This involves the development of a professional and competent group of Kazakhstani specialists capable not only of ensuring the safe handling of PBAs under laboratory conditions, but also of conducting emergency anti-epidemic and anti-epizootic measures to eliminate sanitary-epidemiological and veterinary emergencies, including those arising from natural and technological disasters. 5) Introduction of centralized accounting, registration, and monitoring of the activities of existing laboratories and production facilities that handle and store hazardous PBAs, regardless of their ownership structure or institutional affiliation. Thus, the regulatory acts of the Republic of Kazakhstan adopted during 2020-2023 in the fields of biosafety and biosecurity are consistent with international requirements and WHO recommendations and provide a legal framework for the protection of laboratory personnel.

Conclusions. The practical implementation of the Law «On Biological Safety of the Republic of Kazakhstan» is intended to ensure the national security of Kazakhstan through effective protection of the country against external and internal biological threats. It is also

intended to protect the health of laboratory personnel and the population, as well as the environment, with the aim of preserving it for future generations.

Key words: biosafety; biosecurity; biological risk management; laboratory; pathogen

D. N. Zhetpisbayeva[1, 2], D. A. Klyuyev[1], I. A. Kadyrova[1], N. M. Mazure[2]

RESISTANCE OF PROSTATE CANCER CELLS TO DOCETAXEL OR IRRADIATION AND CHARACTERIZATION OF A NOVEL THERAPEUTIC TREATMENT

[1]«Karaganda Medical University named after P. Pospelov» NC JSC (100008, Republic of Kazakhstan, Karaganda c., Gogolya str., 40; e-mail: info@qmu.kz)
[2]Université Côte d'Azur, INSERM U1065, C3M (06204, France, Nice, 151 route de St Antoine de Ginestière)

Introduction. Prostate cancer is the most frequently diagnosed cancer in men in France and one of the leading cancers in men in Kazakhstan, where 1,359 new cases were registered in 2022. Docetaxel (DTX) and irradiation remain the main therapeutic options for advanced prostate adenocarcinoma; however, their efficacy is limited by the development of resistance. Owing to tumour cell heterogeneity, even when 70-80% of cells are killed, a resistant subpopulation persists, and tumour hypoxia is a key microenvironmental factor that favours the survival of these cells. Calcium signalling regulates proliferation, migration and cell death, and genes encoding members of the store-operated calcium (SOC) channel family are therefore potential targets for overcoming treatment resistance. The aim of this study was to characterize the response of prostate cancer cells to DTX and irradiation under normoxic and hypoxic conditions and to evaluate mibefradil (MBF), an inhibitor of calcium channels including store-operated calcium entry, as a candidate agent to enhance treatment efficacy.

Materials and methods. Human prostate adenocarcinoma cell lines DU145 (androgen-independent) and LNCaP (androgen-sensitive) were cultured under normoxia (Nx, 21% O_2) or hypoxia (Hx, 1% O_2) for 48 h. Cells were treated with DTX (1 – 100 nM) or exposed to irradiation (2 – 10 Gy), and cell viability was assessed. To evaluate drug interaction, cells were treated with combinations of increasing concentrations of DTX and MBF under Nx and Hx, the inhibition of viability was calculated, and synergy was analysed using the zero interaction potency (ZIP) model. The effects of DTX (0.06 – 2 nM) and MBF (2 and 6 µM) were further studied on MSK-PCa3 prostate cancer organoids treated twice over one week, with morphology assessed by bright-field microscopy. Differences were considered statistically significant at $p<0.05$.

Results. DTX reduced cell viability in a dose-dependent manner in both cell lines. In DU145 cells under Nx, viability decreased almost completely at DTX concentrations of 10 nM and above, whereas under Hx approximately 20% of cells remained viable at the same concentrations. LNCaP cells responded to DTX but retained a resistant fraction of cells under both conditions. Irradiation also decreased viability in a dose-dependent manner, and this effect was strongly attenuated by hypoxia: at 10 Gy, the viability of LNCaP cells fell to approximately 15% under Nx but remained around 60% under Hx, while DU145 cells were more radioresistant and retained approximately 70% viability under Hx. In combination experiments, no synergy between DTX and MBF was observed in LNCaP cells under Nx (ZIP score −7.426), and the maximal inhibition (35.5% at 0.3 nM DTX) was not enhanced by MBF. In DU145 cells, the combination showed an additive effect, with a trend towards synergy under hypoxia (ZIP score 0.632 under Nx versus 4.403 under Hx) and synergy regions at higher MBF concentrations. In organoids, DTX caused a dose-dependent loss of organoid integrity, and MBF induced structural alterations.

Conclusion. Hypoxia reduces the efficacy of both DTX and irradiation in prostate cancer cells, confirming its role in treatment resistance, with DU145 cells being the most resistant model. The combination of DTX with MBF showed an additive effect with a tendency towards synergy under hypoxia in DU145 cells, suggesting that targeting the SOC channel family may help overcome

hypoxia-associated resistance. A CRISPR-Cas9 knockout of a SOC channel family gene of interest has been generated and will be used to provide proof of concept that these genes are important for treatment resistance and are targetable.

Key words: prostate cancer; docetaxel; irradiation; hypoxia; store-operated calcium channels; mibefradil

S. A. Zvezhinskiy[1], K. V. Popkov[1], K. V. Senko[1], L. V. Naumenko[2]

IMAGE TEXTURE ANALYSIS – RADIOMICS IN GLIOMA IMAGING

[1]Belarusian state medical university (220083, Republic of Belarus, Minsk c., Dzerzhinsky av., 83; e-mail: bsmu@bsmu.by)
[2]N. N. Alexandrov National Cancer Centre (223040, Republic of Belarus, Minsk c., Lesnoy; e-mail: oncobel@omr.by)

Introduction. Glioma is the most common type of malignant brain neoplasms. Current clinical guidelines include conventional MRI an CT of brain followed by diagnostic biopsy to define tumor immunohistochemical and genetic characteristics. But this procedure is quite invasive and is associated with such surgical complications as infection and hemorrhage. Moreover, only limited part of solid component of the tumor can be investigated through this method. Preoperational estimation of tumor aggressiveness presents a challenging problem for radiologists and neurosurgeons due to its importance in surgical corridor choice, clinical answer to radiation or chemotherapy. Radiomics is a promising tool in this field, because it allows multimodal analysis of selected region of interest presenting numerous types of parameters, which could be helpful in glioma management.

Materials and methods. Systemic review of literature linked to radiomics application in glioma management was performed. Three of the most relevant scientific electronic databases (PubMed, Web of Science, Google Scholar) were comprehensively explored and used to build the search.Key words for search were: glioma, radiomics, IDH-status, MGMT, Ki-67, p53, ATRX, AUC.

Results. Calabrese et al. reported a high prognostic efficacy of models predicting IDH-mutation status (AUC=0,97), MGMT-methylation status (AUC=0,77) and ATRX (AUC=0,97). For such common markers as p53, CDKN2A/B, AUC values were 0,86 and 0,79, respectively. 3D-segmentation of tumor was performed using PyRadiomics, contrast-enganging as well as non-enhancing part of tumor were assessed to calculate texture features. Problem of multicollinearity was excluded due to Recursive Feature Elimination algorithm, which choose 32 out of 5300 radiologic features to predict each biological marker. Ni et al. performed a comprehensive research dedicated to Ki-67 prognosis. Eight different Machine Learning algorithms (Logistic regression (LR), naive bayes, decision tree, gradient boosting tree, and support vector classification (SVM), random forest (RF), XGBoost, and LightGBM) were performed with highest AUC values 0,88 defining Ki-67 value of the tumor. For this study, 24,455 radiomic features were extracted from each patient's MRI, combination of LASSO-regression and Recursive Feature Elimination was used only useful and avoid multicollinearity phenomenon.

Conclusion. Radiomics is the new step in glioma diagnostics and management. This method shows high prognostic values in distinguishing neoplasms with different immunohistochemical and genetic type. Combined with Machine Learning algorithms to choose only significant and helpful features it allows a neuroradiologist to estimate tumor characteristics more accurately by using only MRI, which is relatively cheap, radiation-free diagnostic method. However, it cannot

replace intraoperative biopsy, but can serve as important tool in patient's preliminary distribution and to define which markers are more likely to be tested.

Key words: glioma, radiomics, texture analysis, segmentation, machine learning

D. E. Yakobson[1], M. N. Zharkov[1]

ACUTE TOXICITY AND MORPHOLOGICAL SAFETY OF Fe_3O_4 AND Zn-Mn FERRITE MAGNETIC NANOPARTICLES WITH DIFFERENT COATINGS

[1]National Research Ogarev Mordovia State University (430005, Russia, Saransk, Bolshevistskaya str., 68, e-mail: ykbsn@mail.ru)

Introduction. Magnetic nanoparticles are promising agents for local antitumor technologies, including magnetic hyperthermia. Their biomedical use requires assessment of systemic safety because in vitro cytotoxicity does not fully predict the organism-level response. The biological effects of magnetic nanoparticles can depend not only on the composition of the magnetic core but also on the surface coating and route of administration. The aim of this study was to compare the acute toxicity and systemic safety of Fe_3O_4- and $Zn_{0.2}Mn_{0.8}Fe_2O_4$-based nanoparticles coated with oleic acid/sodium oleate or amino-functionalized silica.

Materials and methods. Four nanoparticle formulations were studied: Fe_3O_4@OA, $Zn_{0.2}Mn_{0.8}Fe_2O_4$@OA, Fe_3O_4@SiO_2-NH_2, and $Zn_{0.2}Mn_{0.8}Fe_2O_4$@SiO_2-NH_2. Male BALB/c mice aged 40-45 days and weighing 18-24 g were used. Acute toxicity after a single intraperitoneal injection was evaluated at doses of 274-4896 mg/kg with 14-day observation and LD50 calculation by probit analysis. Intramuscular tolerability was assessed at 1020 mg/kg. Hematological and biochemical blood parameters and the morphology of the injection-site muscle, liver, spleen, kidneys, and lungs were evaluated on days 2, 14, and 90 after intramuscular administration at 256 and 1020 mg/kg. Differences were considered significant at $p<0.05$.

Results. After intraperitoneal administration, LD_{50} values were 904 mg/kg for Fe_3O_4@OA, 1145 mg/kg for $Zn_{0.2}Mn_{0.8}Fe_2O_4$@SiO_2-NH_2, and 2955 mg/kg for $Zn_{0.2}Mn_{0.8}Fe_2O_4$@SiO_2-NH_2. The LD_{50} for Fe_3O_4@SiO_2-NH_2 was not reached at the maximum tested dose of 4896 mg/kg. Thus, acute toxicity was influenced more strongly by surface coating than by magnetic core composition. After intramuscular administration of 1020 mg/kg, no deaths, marked behavioral abnormalities, or significant body weight loss were observed. Most hematological and biochemical parameters remained within the reference intervals. Individual laboratory changes were not accompanied by marked morphological signs of organ injury. Liver architecture was preserved in all groups without widespread necrosis, pronounced inflammatory infiltration, or gross parenchymal damage. The structure of the spleen also remained preserved without massive hemorrhage or necrosis. Renal glomeruli and tubules were preserved throughout the observation period, while only focal interstitial cellular infiltrates were observed in individual fields on day 90. The general alveolar structure of the lungs remained preserved. Focal peribronchial or perivascular cellular infiltrates were occasionally detected, without massive hemorrhage or widespread alveolar injury. No marked tissue damage or inflammation was detected in the muscle at the injection site.

Conclusion. The acute toxicity of the investigated magnetic nanoparticles depended mainly on the surface coating and route of administration. The SiO_2-NH_2 coating was associated with lower acute toxicity after intraperitoneal administration. All formulations showed good tolerability after local intramuscular administration, with no mortality and no pronounced systemic or morphological toxicity at the studied doses.

Key words: magnetic nanoparticles; acute toxicity; magnetite; manganese-zinc ferrite; silica coating; oleic acid

CONTENTS

Aitkenova A. A., Atazhanova G. A.
Biological effects of an ultrasound-assisted ethanolic extract of *Iris scariosa* L. in yeast and *Artemia salina* bioassays…….. 4

Arzakulova M. M., Tokashbayeva D. A., Omertayeva D. E.
Metabolomic biomarkers of severe chronic hypertension in pregnancy: associations between purine intermediates and Beta-2-microglobulin……..... 5

Biyaliev E. B., Ivasenko S. A., Korona-Glowniak I., Marchenko A. B.
Development of a new antibacterial agent for the treatment of pneumococcal diseases based on biologically active substances of *Thymus crebrifolius* Klok…… 6

Darmani Z., Shahzaib M., Modabber M. H., Haider S., Myrzakhanova M.
The effect of virtual reality on students' attention and visual memory……..... 7

Duisegali D., Fadin M., Yegorov S., Strochkov V., Lavrinenko A., Parakhina V., Sandybayev N.
Impact of empiric antibiotics on microbial diversity and antimicrobial resistance in pneumonia……..... 8

Hramyka A. V., Zvezhinskiy S. A., Baroski A. A., Davidyan A. V.
Use of machine learning to predicт recurrence after third ventriculostomy…….. 9

Izerskaya M. S., Dildabekova L. A.
Enzymes as biological catalysts and their significance in the child's organism…… 11

Kalkenova A. T., Mendibayeva A. Zh., Shestakov D. V., Shakeyev K. T., Zeinidenov A. K.
Spectroscopic analysis of saliva samples using fluorescence and FTIR spectrometry for cervical cancer detection…… 12

Kazbekova A., Sagadinov S., Yegorov S.
Detection of bacteriophage signatures in targeted sequencing data from sputum samples of patients with pneumonia in Kazakhstan……. 13

Kelgali G. K., Aldabergen I. E., Mendibayeva A. Zh., Aimukhanov A. K., Zeinidenov A. K.
Spectral-luminescent characteristics of saliva in lung cancer diagnosis…… 14

Khan O. I., Olkhov A. A., Karpova S. G.
Non-woven fibrous materials based on polylactide and polycaprolactone for medical applications……. 16

Kosherov O. K., Ivasenko S. A., Kacergius T.
Antibacterial and antibiofilm activity of thymus crebrifolius klok. Extracts against *Streptococcus mutans*……. 17

Manish G.
Regional trends in multidrug/rifampicin-resistant tuberculosis: analysis of WHO data from 2015 – 2024…… 18

Mirsaidullaev M. M., Mamasoliev N. S.
Transnosological comorbidity in reproductive-age women with ischemic heart disease: results of population screening in Namangan…….. 19

Mirsaidullaev M. M., Mamasoliev N. S.
Comorbid profile and pharmacotherapeutic features of ischemic heart disease in reproductive-age women……. 20

Muzapparova D., Dildabekova L. A.
Artificial intelligence in the diagnosis and treatment of children: from chemical analysis to personalized medicine……. 21

Myrzakhanova M. N.
Current advances in virtual autopsy using integrated visualization technologies…… 22

Nikandrova A. A., Komarova E. S., Lukianov D. A., Zakalyukina Y. V., Alferova V. A., Chernyshova A. P., Biryukov M. V., Sergiev P. V.
Screening and genomic analysis of antibiotic-producing streptomyces and characterization of antibacterial mechanisms…….. 24

Okassov D. B., Ivasenko S. A., Seité P., Vannier B., Marchenko A. B.
Antitumor activity of *Thymus serpyllum* L. Extracts and their polyphenolic profiles….. 25

Parshutina A. A.
The effect of dressings with granulated sorbent and chlorhexidine-dioxidine mixture on wound defects treatment duration in patients with diabetic foot syndrome at the outpatient stage…….. 26

Sabyrbekova A., Worth A., Faizov B., Tulchinsky E., Kriajevskaia M.
Bladder cancer organoids as a platform for transcriptomic analysis of tumor development and treatment response…… 27

Sagadinov S. O., Kazbekova A. A., Yegorov S. V.
Conservation of surface protein targets for structure-guided drug development in clinical isolates from Kazakhstan……. 29

Satken K. S., Ablaikhanova N.
Circulating miR-20a as a biomarker for early detection of non-small cell lung cancer…… 30

Shashkova V. N., Tyulegenova D. S., Malvenova A. A., Kurmangazhina B. K., Tulebayev Ye. A.
Drug encapsulation technology……..... 31

Sheyda E. V., Duskaeva A. G.
Dose-dependent effect of zinc on rat activity and behavior……. 32

Stabayeva L., Mergazina M., Kamyshanskiy Ye., Amirbekova Zh.
Myxoid histophenotype of the cervical stroma as a potential morphological marker of high-risk CIN progression…… 34

Starodubtseva D. A., Panov S. A., Danayeva D. Zh.
Changes in oxidative stress and mitochondrial activity markers during personalized metabolic correction: a retrospective case series…… 35

Tabakchi O. E., Mukhametova D. D., Odintsova A. Kh., Abdulganieva D. I.
Ultrasound imaging of skeletal muscles in the comprehensive diagnosis of sarcopenia in patients with inflammatory bowel disease…….. 36

Takhauova L. R., Takhauov A. R., Smagliy L. V.
Proteomic profiling of tear fluid to identify molecular signatures of changes in ocular surface status…… 37

Turabayeva B. M., Ospanova M. E., Baltabayeva T. S., Zhangazieva K. H., Abdrakhmanova S. A.
Preparation of apheresis product for CAR-T therapy: experience of the scientific and production center for transfusiology…… 38

Utepov P. D.
Organization of a biosafety system for laboratory personnel…….. 39

Zhetpisbayeva D. N., Klyuyev D. A., Kadyrova I. A., Mazure N. M.
Resistance of prostate cancer cells to docetaxel or irradiation and characterization of a novel therapeutic treatment……. 41

Zvezhinskiy S. A., Popkov K. V., K Senko. V., Naumenko L. V.
Image texture analysis – radiomics in glioma imaging……..... 42

Yakobson D. E., Zharkov M. N.
Acute toxicity and morphological safety of Fe_3O_4 and Zn-Mn ferrite magnetic nanoparticles with different coatings…… 43